Full-field Phase Imaging in practice and the impact of improved coherence

Rajmund Mokso

Solid Mechanics Department & MAX IV Laboratory

Lund University

Outline

I. Introduction to full-field imaging in the Fresnel regime
   I. Overview of routines

II. Imaging at various scales of coherence
   I. Lab systems
   II. Synchrotron
   III. XFEL

III. Challenges

IV. Perspectives

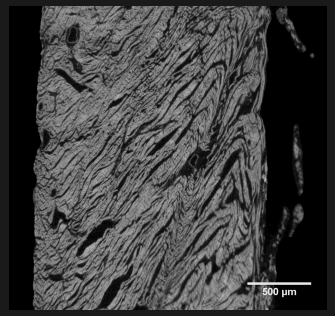

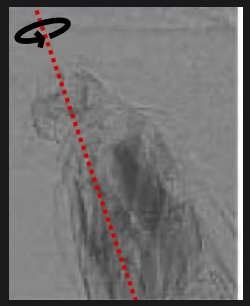

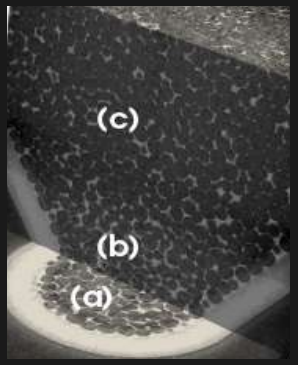

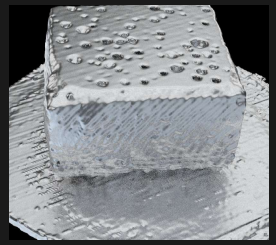

Rajmund.Mokso@maxiv.lu.se

Tomographic microscopy at synchrotron

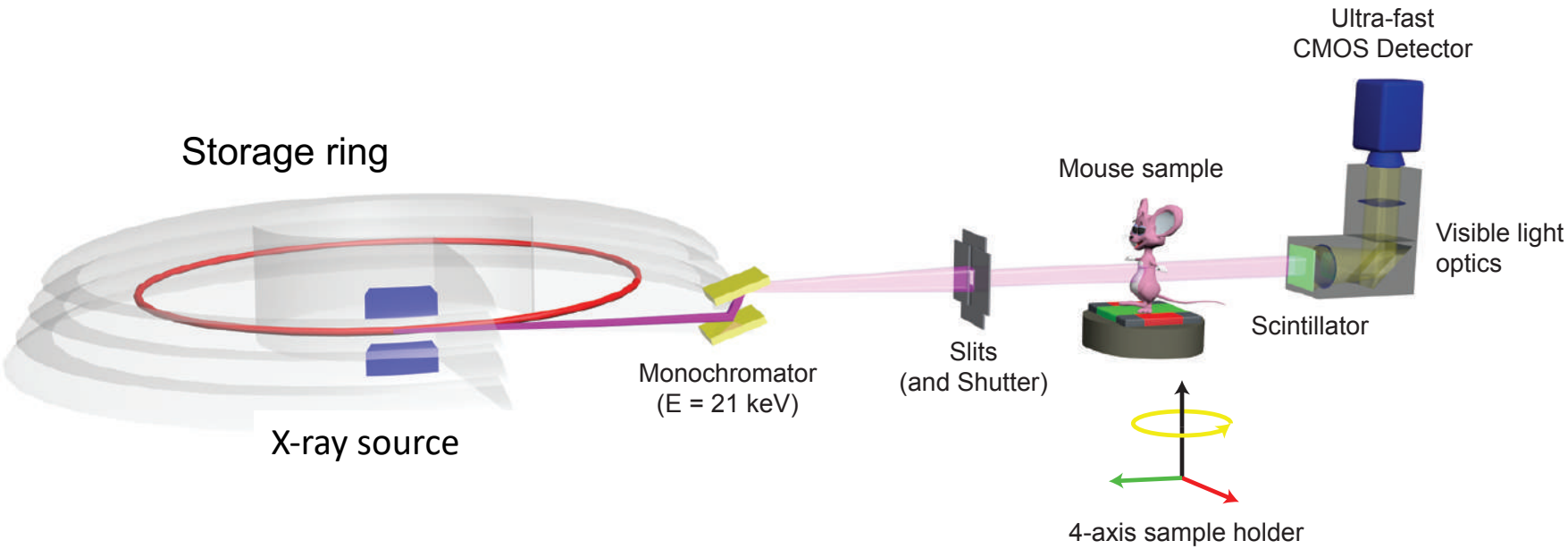

Radiographic projection clinics

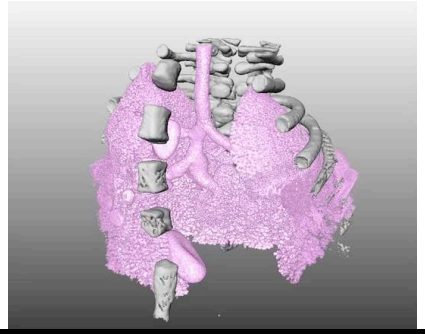

Tomographic reconstruction Synchrotron

Pixel size: 11 -> 0.3 µm

FOV: 22 x 22 -> 1 x 1 mm^2

Projections: 300–2000

Exposure times: 0.1–300 ms

Total scan time: 0.05 to 500 s

Hierarchical imaging of biological samples

Pre-clinical imaging and therapy
(in vivo, medium resolution >30 um, low dose, large beam , large FOV)

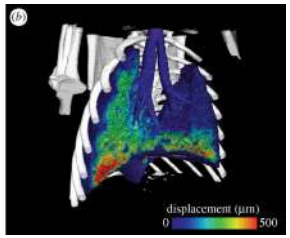

Longitudinal in vivo

The whole organ

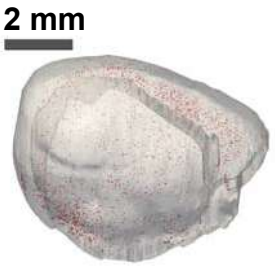

Down to a micrometer resolution
(rarely in vivo, high resolution ~ 1um, higher dose, small FOV)

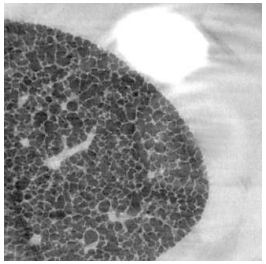

Acute in vivo

Zooming into organs

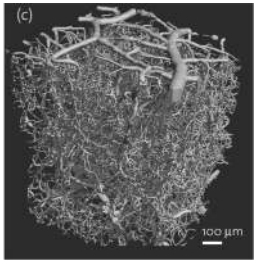

Nano-scale imaging beamlines
(fixed tissue, resolution ~ 100nm, high dose, small samples ~100um)

Bronchial wall

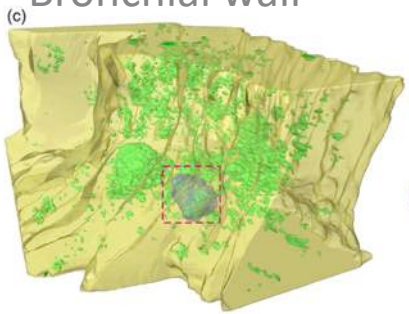

Fixed tissue

Cell level

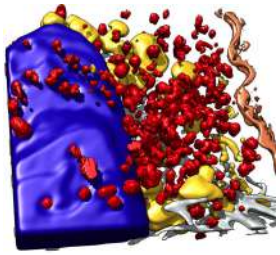

100µm mGy 0.5m 0.1 s

Spatial resolution

Radiation dose

Field of view (sample size)

3D scan time

10nm MGy 100µm 1 h

3 orders of magnitude in spatial resolution

Phase contrast in free space propagation

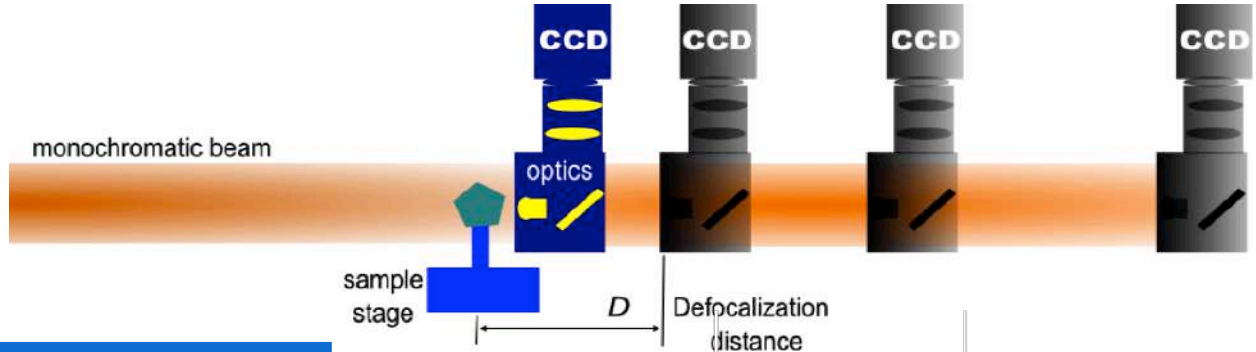

$$U_D(x) = U_0(x) \otimes \sqrt{\frac{-i\pi}{\lambda . D}} . e^{\frac{i\pi}{\lambda . D} . x^2}$$

propagator

Born, M., and E. Wolf, 1990, Principles of Optics

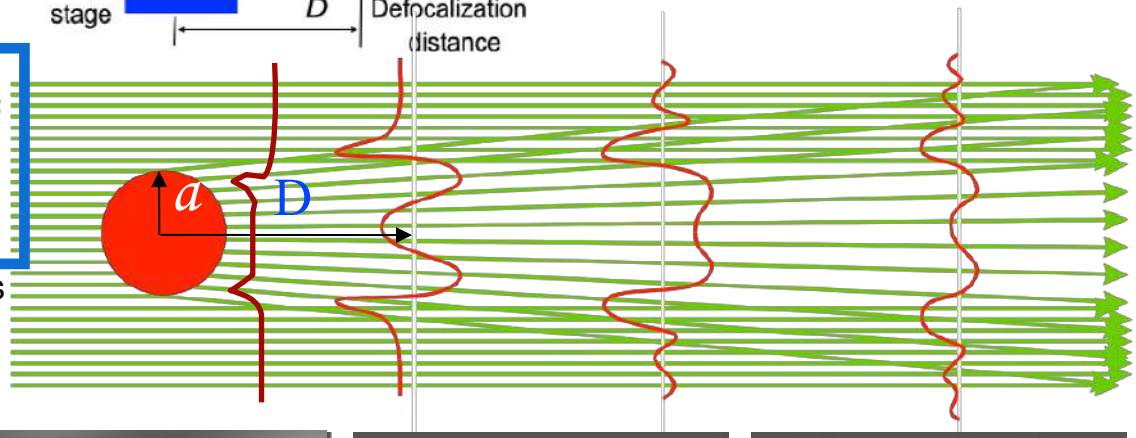

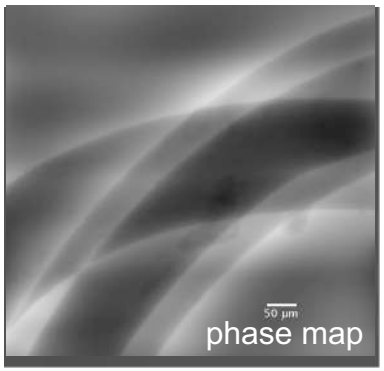

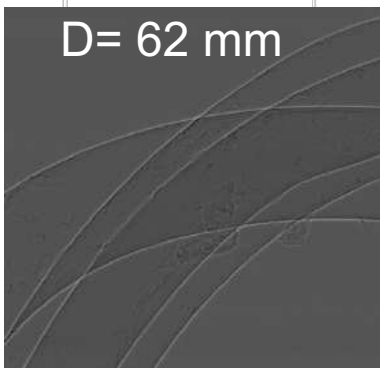

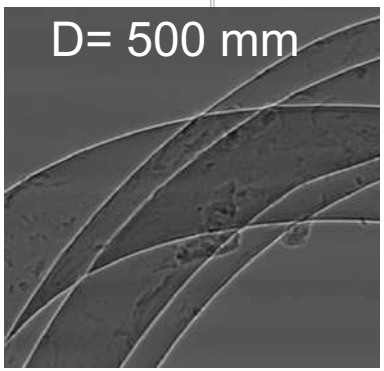

Three phase fibers

Fresnel diffraction
Partially coherent illumination

$$\varphi(f) = \frac{\sum_m \sin(\pi \lambda D_m f^2) I_m(f)}{\sum_m 2\sin^2(\pi \lambda D_m f^2)}$$

Cloetens et al. J. Phys. 1999

Rajmund.Mokso@maxiv.lu.se

Free space phase imaging

Linear scenarios for near-field phase retrieval:

Transport of Intensity Equation (Small propagation distance)

$$-k\frac{I(\boldsymbol{x};z)-I(\boldsymbol{x};0)}{z}=\nabla I(\boldsymbol{x};0)\nabla\psi(\boldsymbol{x})+I(\boldsymbol{x};0)\Delta\psi(\boldsymbol{x})$$

Teague, J. Opt. Soc. Am. 73, 1434 (1983)

Contrast Transfer Function (Weak scattering and absorption object)

$$I_D(\boldsymbol{f}) = \delta_{Dirac}(\boldsymbol{f}) - \underbrace{2\cos(\pi\lambda D\boldsymbol{f}^2)}_{\text{amplitude contrast factor}} . B(\boldsymbol{f}) + \underbrace{2\sin(\pi\lambda D\boldsymbol{f}^2)}_{\text{phase contrast factor}} . \varphi(\boldsymbol{f})$$

Guigay, Optik, 1977

Combination different distances

D_m least squares minimisation

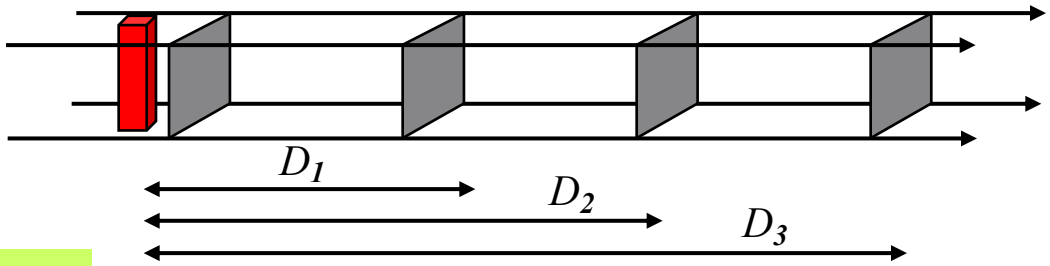

$$\tilde{\varphi}(f)=\frac{1}{2\Delta}\sum_{m=1}^{N}\left[\mathrm{A}\sin(\beta_m)-\mathrm{B}\cos(\beta_m)\right]\tilde{I}_m^{\exp}$$

$$\tilde{B}(f)=\frac{1}{2\Delta}\sum_{m=1}^{N}\left[\mathrm{A}\cos(\beta_m)-\mathrm{C}\sin(\beta_m)\right]\tilde{I}_m^{\exp}$$

direct method

$$\mathrm{A}=\sum_m \sin(\beta_m)\cos(\beta_m)$$

$$\mathrm{B}=\sum_m \sin^2(\beta_m)$$

$$\mathrm{C}=\sum_m \cos^2(\beta_m)$$

$\Delta = \mathrm{B.C\text{-}A}^2$

$\beta_m = \pi\lambda D_m f^2$

Cloetens, 1996 & 1999

Phase (contrast) tomography

Finding the phase of the object (real part of the refractive index)

$$I_D(\mathbf{x}) = \left|\mathrm{FRT}_k[\mathrm{T}_{A,\varphi}(\mathbf{x})]\right|^2$$

$$\phi(\mathbf{x}) = \arg\min_{\phi} \left\| \left|\mathrm{FRT}_k[\mathrm{T}_{A,\phi}(\mathbf{x})]\right|^2 - I_D(\mathbf{x}) \right\|^2$$

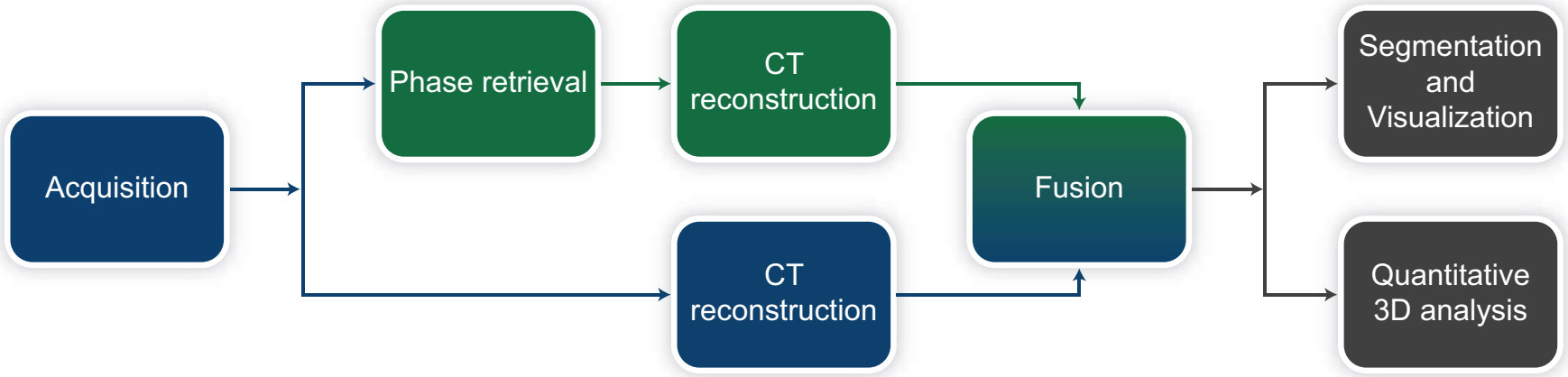

Motivation to utilize phase in full-field imaging

Contrast enhancement

- Improve CNR == less noisy images == reliably image interpretation / segmentation

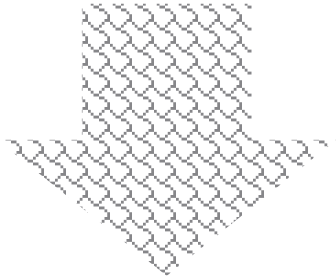

- reduce dose enables high resolution in-situ and in vivo imaging

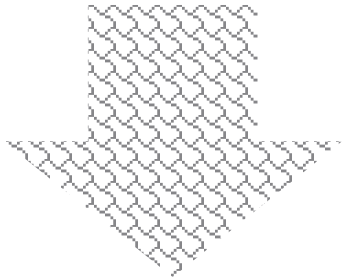

- enhance acquisition speed to avoid motion blur due to sample movement

Rajmund.Mokso@maxiv.lu.se

Handling coherence in full-field imaging

How do we practically handle interference of coherent beams in full-field imaging?

- Retrieve the phase and attenuation deploying CTF or TIE based algorithms -> used mainly in nanoimaging with projection microscope
- Filter the projections with the Paganin filter to obtain the projected density -> very successful at beamlines because it is robust and simple
- Use the edge enhanced image -> often suitable for visual analysis
- We simply remove fringes to get clear attenuation image (e.g. decoherer on beamlines / Bronikov aided correction for lab sources)

Rajmund.Mokso@maxiv.lu.se

Starting with low coherence

Lab microtomograph

4D IMAGING LAB@LTH

MAX IV

SoftiMAX

Soft X-rays
(in construction -> 2020)

NanoMAX

The nanofocus beamline
(users in 2017)

DanMAX

Imaging & diffraction
(in construction -> 2020)

2016 2017 2018 2019 2020

@maxiv.lu.se

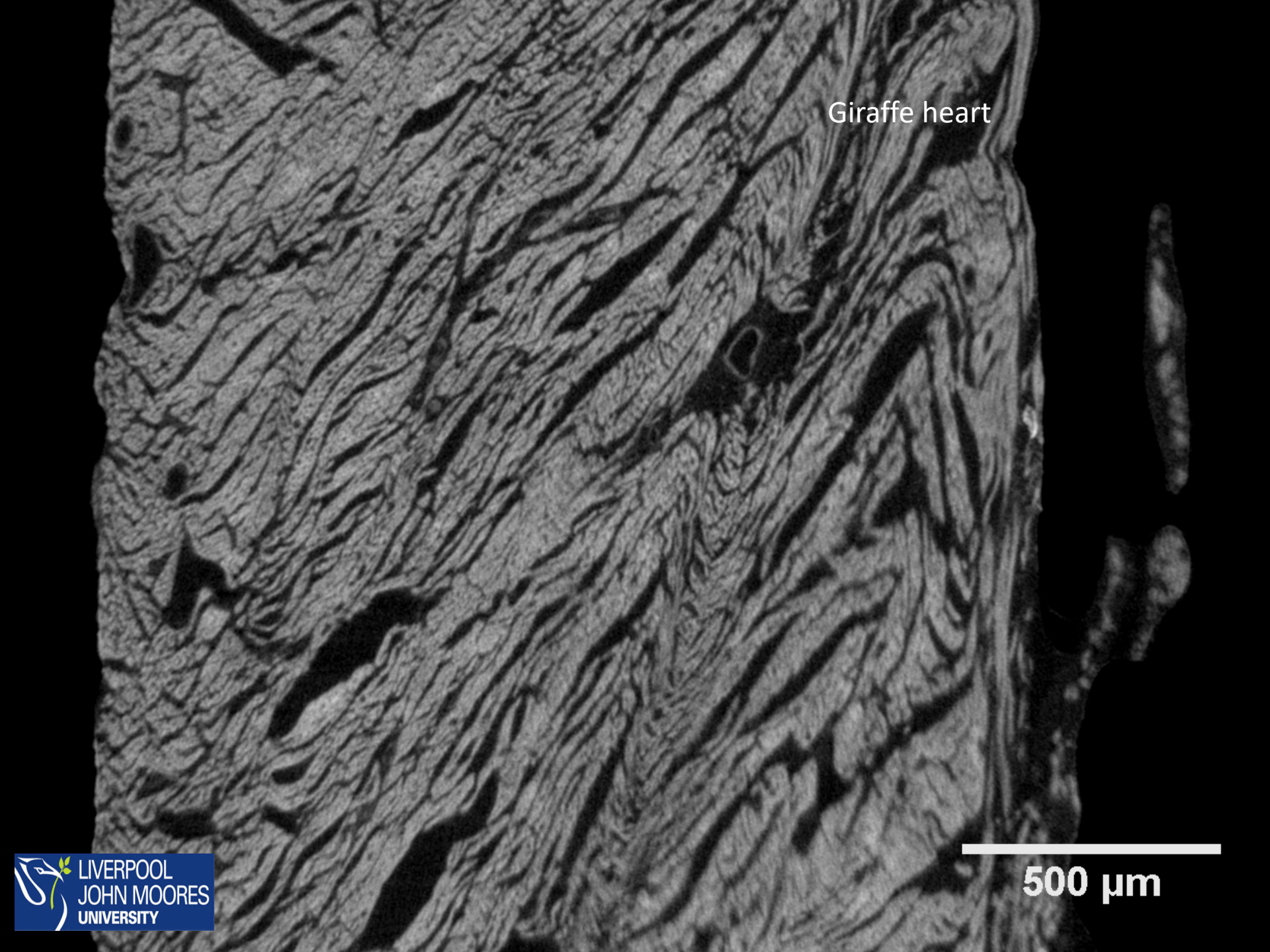

LIVERPOOL JOHN MOORES UNIVERSITY

Little coherence: lab sources

Edge enhancement vs. Paganin filtering for Versa 520

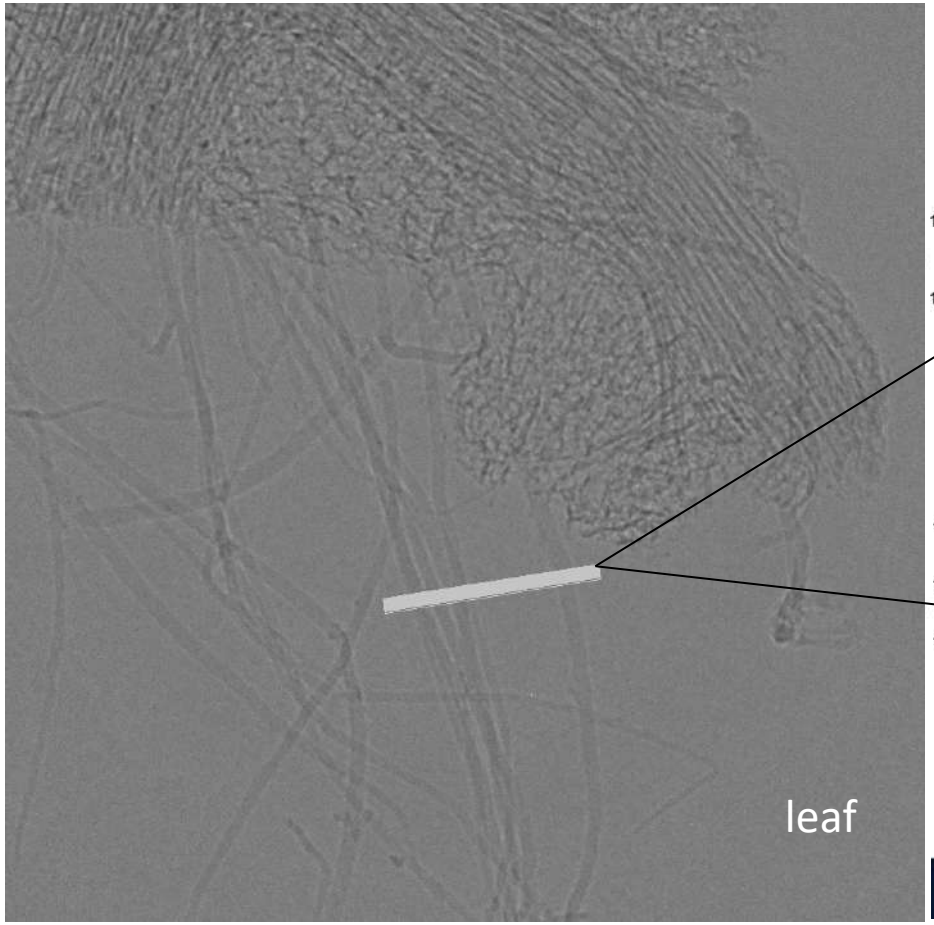

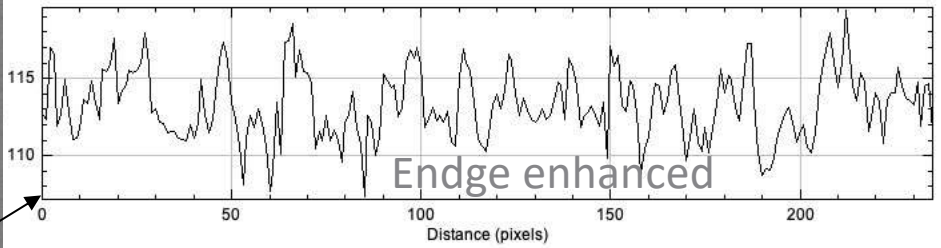

Profile plot

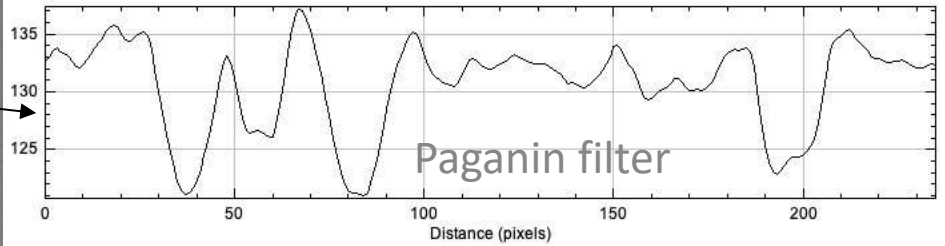

F. Mattsson, Master thesis, LTH

Exposure time = 1s, pixel size = 500 nm

60 kV (+filter) -> $E_{effective}$ ~ 30 keV

Rajmund.Mokso@maxiv.lu.se

Medium coherence

Standard imaging beamline

Phase tomography

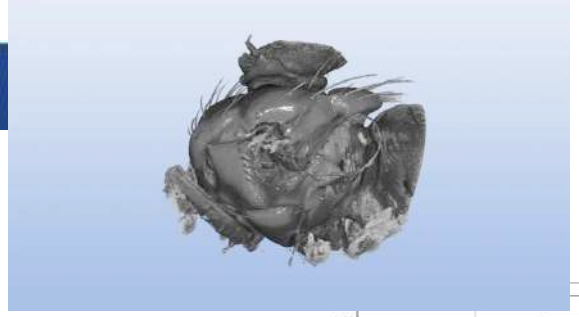

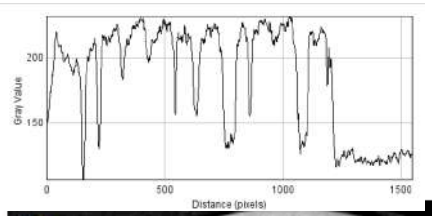

- Refractive index n $n = 1 - \delta + i\beta$ $\quad \delta >> \beta$

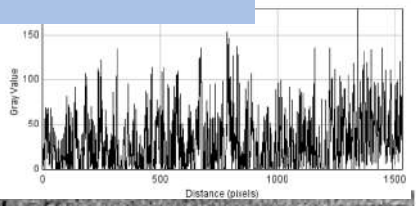

fast tomography
30% of detector dynamic range

flight muscles of a fly

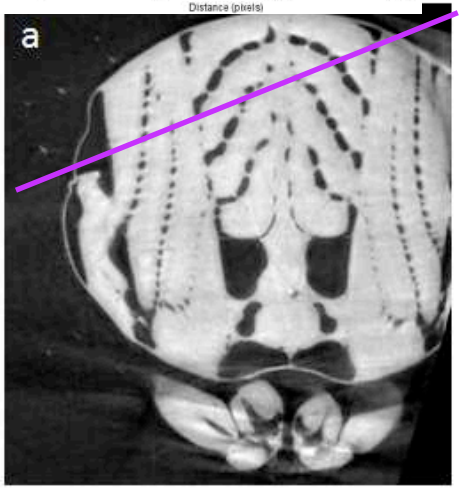

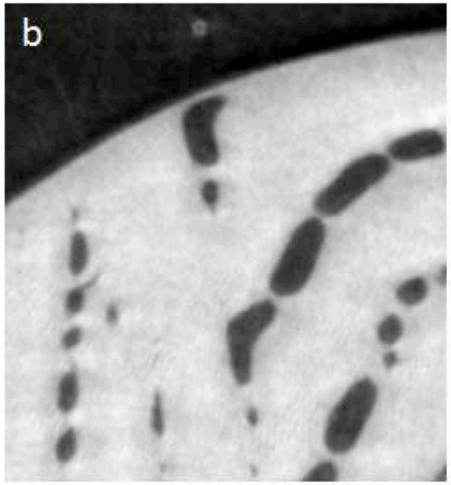

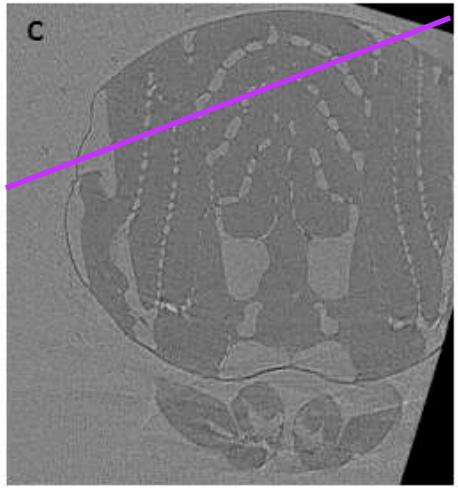

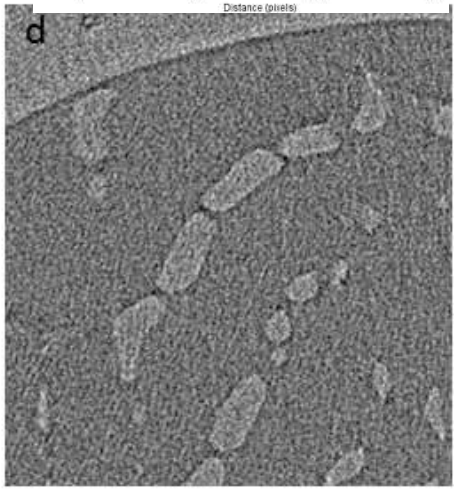

phase map

absorption & edge

Phase tomography

Phase contrast tomography

Mokso et al. J. Phys. D, 2013

Image quality vs. radiation damage

2.9 µm pixel-size optics

G. Lovric et al., J. Appl. Cryst. 46 (4) 2013

901 projections	901 projections	901 projections	361 projections
		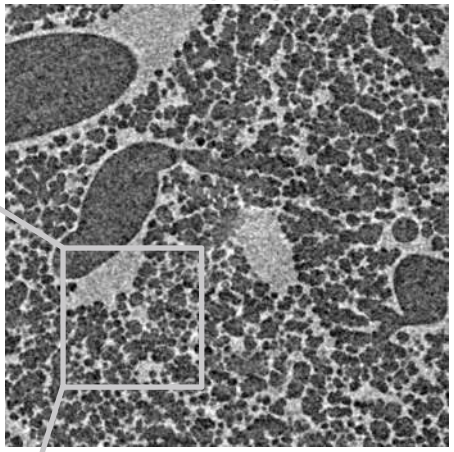	
		0.24 s	0.17 s
		CNR	CNR
		2.3	1.5
		Entrance dose	Entrance dose
		12 Gy	9 Gy

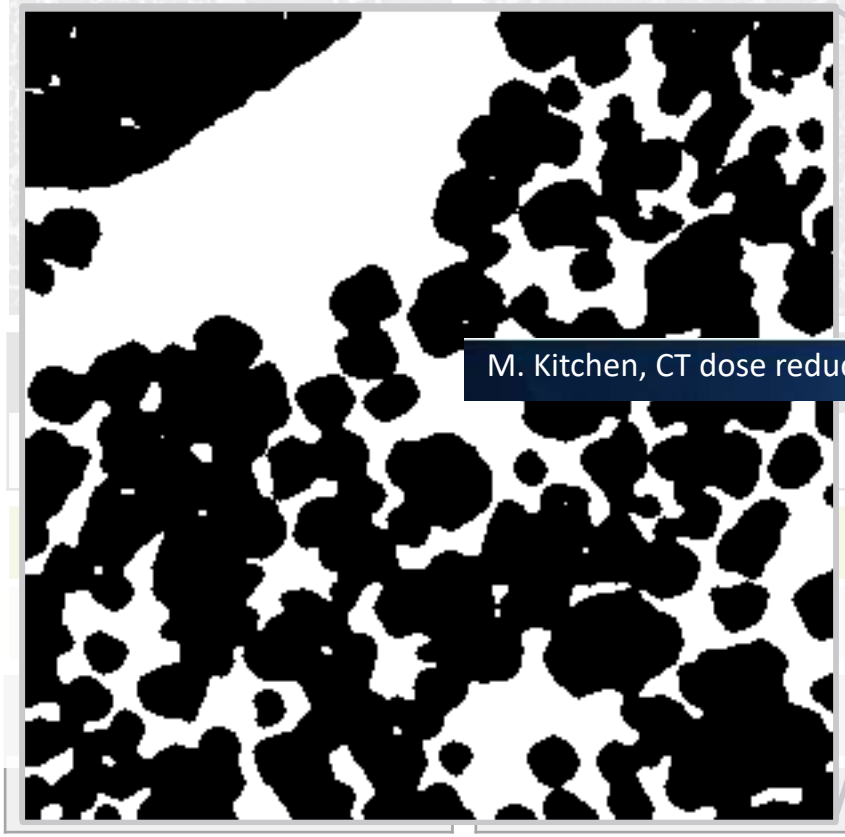

M. Kitchen, CT dose reduction factors in the thousands using X-ray phase contrast, Sci. Rep. 7 (2017)

Lung alveoli microstructure in vivo

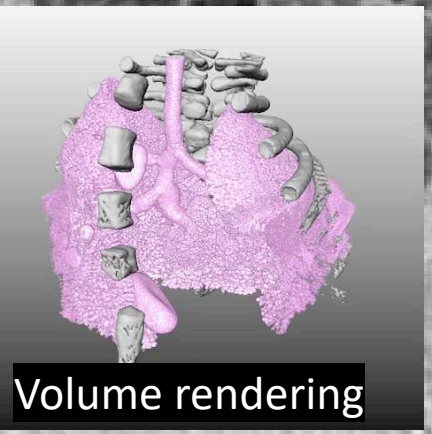
Volume rendering

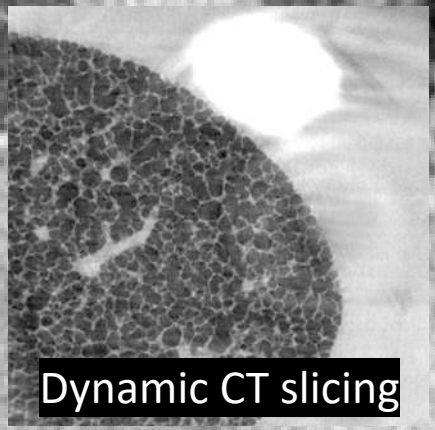
Dynamic CT slicing

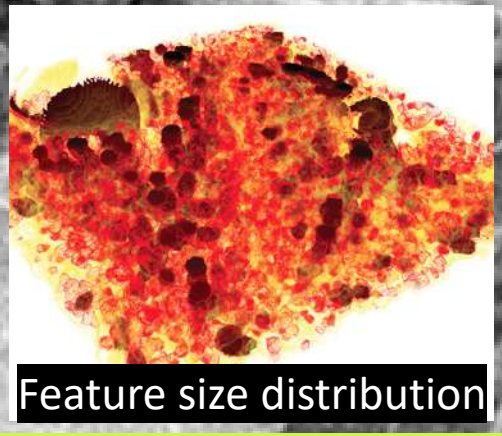
Feature size distribution

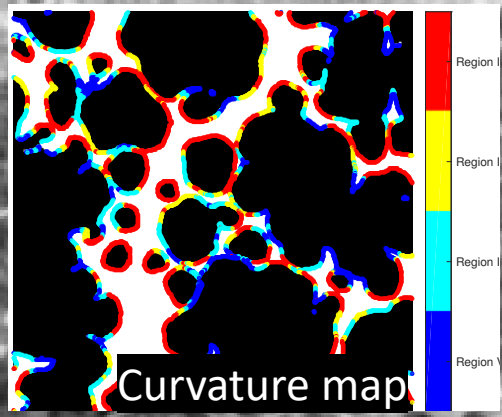

Curvature map

In vivo tomographic microscopy

Lovric et al. Sci. Rep. 2017

1 mm

Highly coherent beams

Coherent imaging beamline

Nanoimaging with focused beam

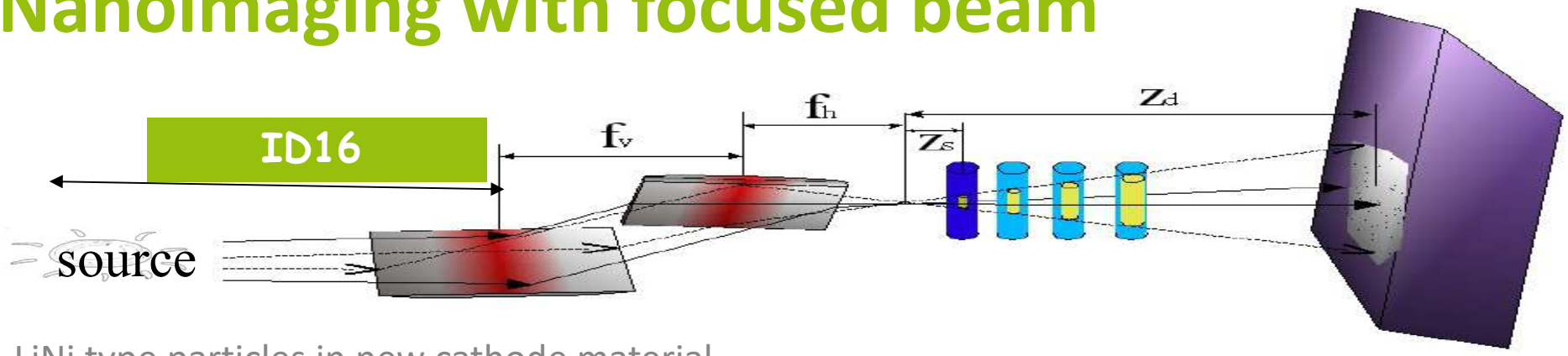

LiNi type particles in new cathode material

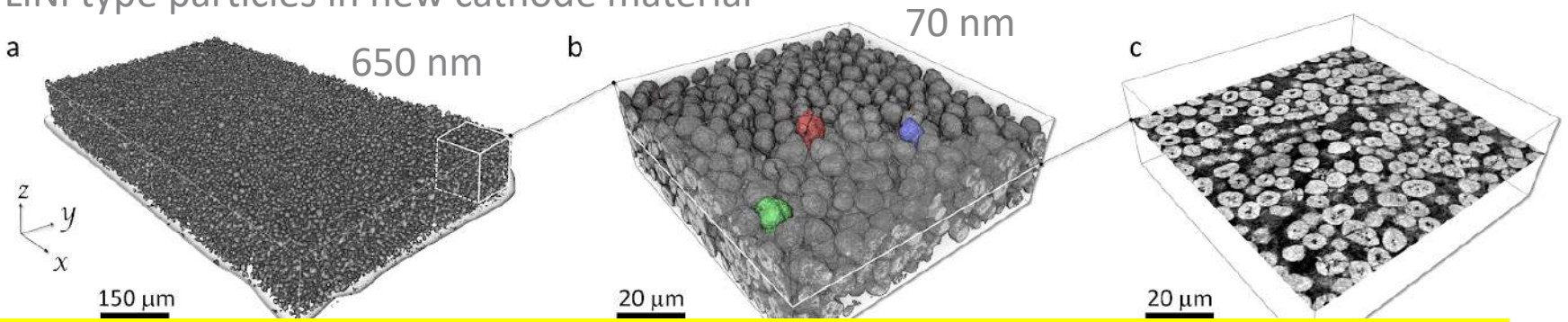

- Hierarchical morphology of secondary particles in Li-rich cathode materials.
- Develop at longer charging time 50cycle >10cycle

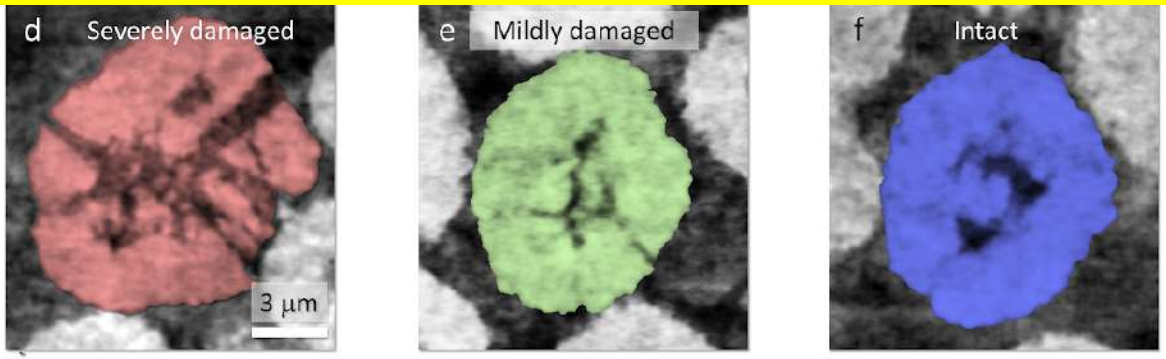

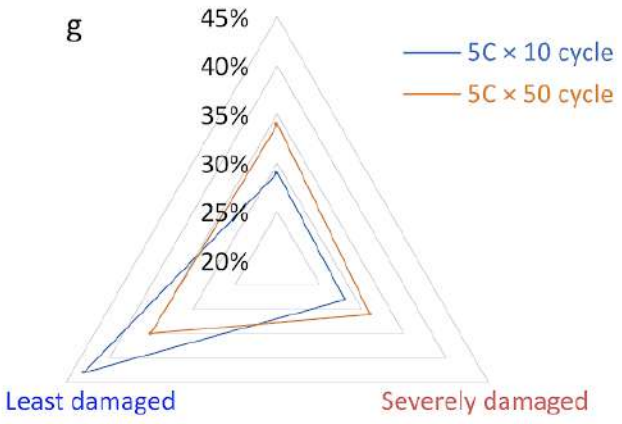

Y. Yang, Y. Liu, et al., Adv. Energy Mater. (2019)

Quantification of Heterogeneous Degradation in Li-ion Batteries

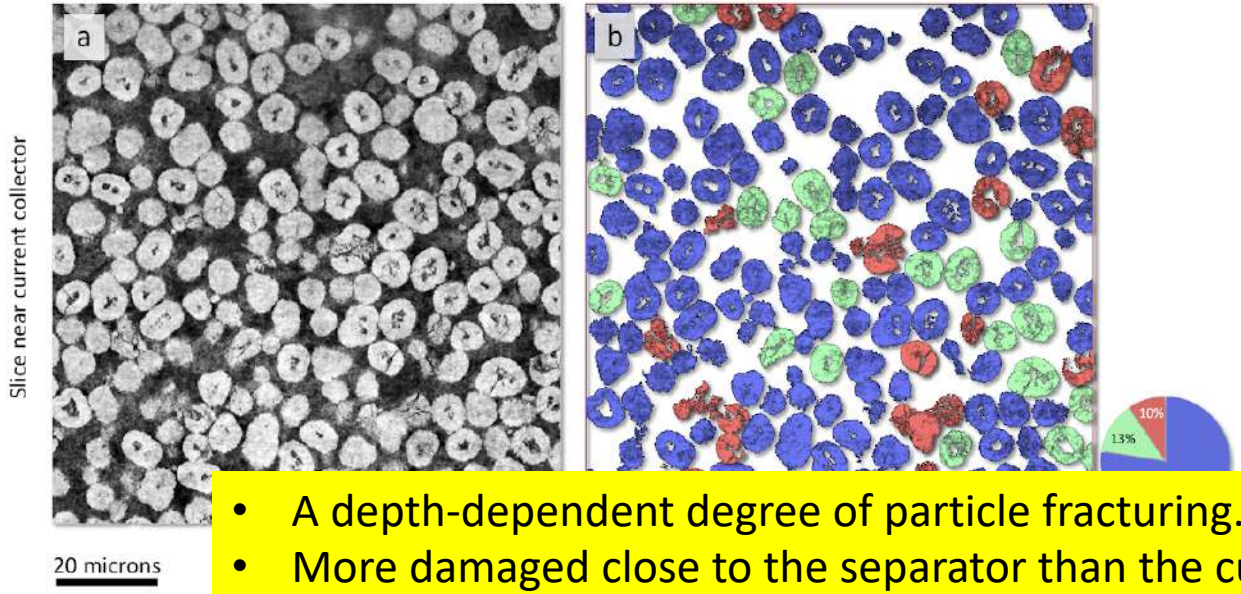

- A depth-dependent degree of particle fracturing.
- More damaged close to the separator than the current collector.

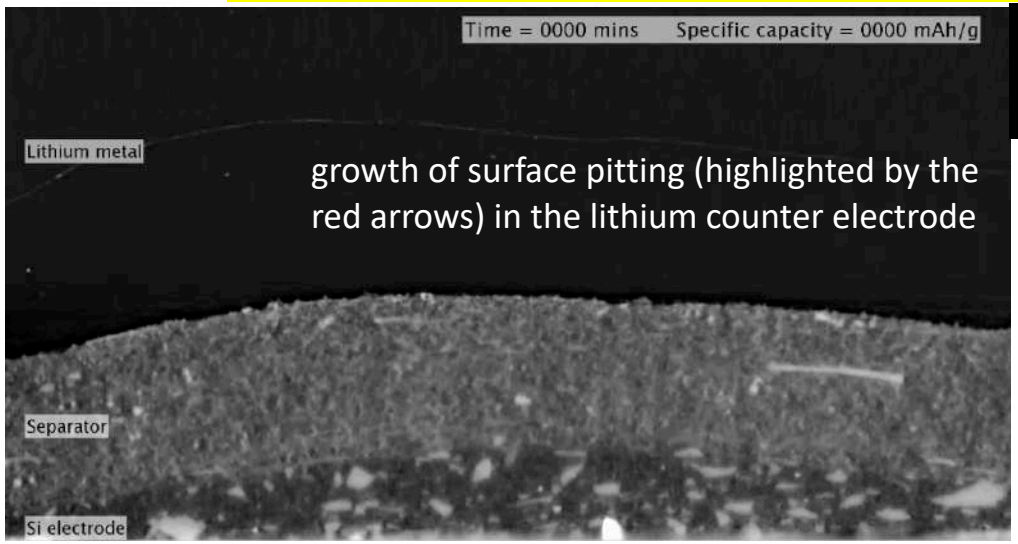

Y. Yang, Y. Liu, et al., Adv. Energy Mater. (2019)

In situ degradation of Si electrode / TOMCAT, SLS

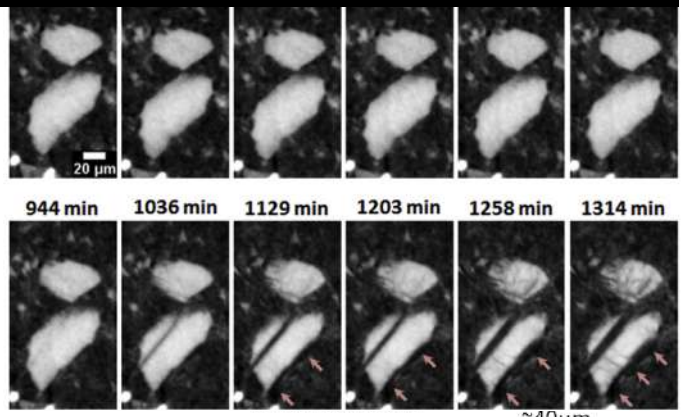

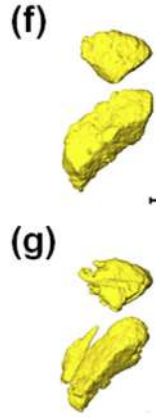

Taiwo, et al., J. Power Sources. 342 (2017)

Development in phase retrieval algorithms

Working towards a more robust phasing tool

Direct model in phase retreival, CTF

$$\tilde{I}_D(\mathbf{f}) = \delta(\mathbf{f}) - 2\cos\left(\pi\lambda D|\mathbf{f}|^2\right)\tilde{B}(\mathbf{f}) + 2\sin\left(\pi\lambda D|\mathbf{f}|^2\right)\tilde{\phi}(\mathbf{f}),$$

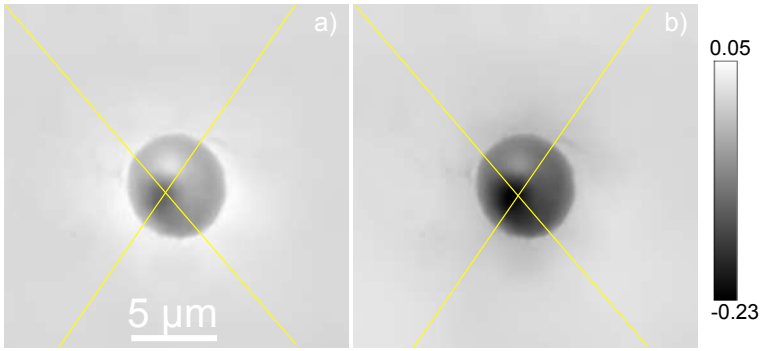

Fig. 6. Phase map of a red blood cell obtained through a) standard regularization and b) Bayesian inference.

Solution by minimization of the Euklidian distance

$$\hat{\mathbf{x}} = \arg\min_{\mathbf{x}} \|\mathbf{y} - \mathbf{H}\mathbf{x}\|^2 = \arg\min_{\mathbf{x}} J_{LS}(\mathbf{x})$$

System matrix

Needs regularisation:

$$J(\mathbf{x}) = \|\mathbf{y} - \mathbf{H}\mathbf{x}\|^2 + \lambda_R \Delta(\mathbf{x}, \mathbf{x}_0)$$

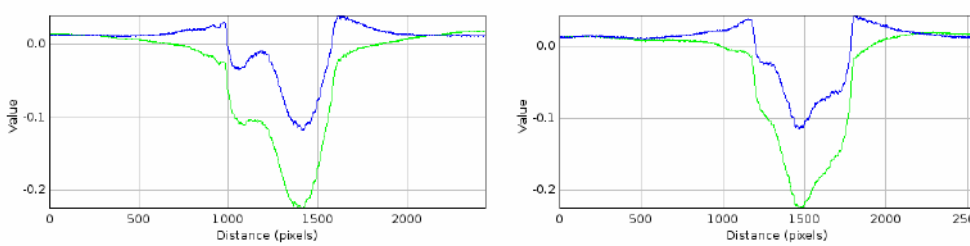

Research Article Vol. 26, No. 25 | 10 Dec 2018 | OPTICS EXPRESS 32847
Optics EXPRESS

Robust determination of the regularisation parameter under Bayesian framework

Unsupervised solution for in-line holography phase retrieval using Bayesian inference

FLORIN FUS,[1,2,*] YANG YANG,[1] ALEXANDRA PACUREANU,[1] SYLVAIN BOHIC,[1,2] AND PETER CLOETENS[1]

Phase retrieval with compressed sensing

- Phase problem:

$$\bar{\phi} = \min_{\phi}[|\boldsymbol{H}\phi - I|^2 + \eta R(\phi)], \text{ where } I = \boldsymbol{H}\phi;$$

- Contrast Transfer Function

Weak scattering absorption object

$$\hat{I}_z(\boldsymbol{f}_x) = 2\hat{\psi}(\boldsymbol{f}_x)sin(\pi\lambda z|\boldsymbol{f}_x|^2) - 2\hat{B}(\boldsymbol{f}_x)cos(\pi\lambda z|\boldsymbol{f}_x|^2)$$

$$\boldsymbol{H} = \mathcal{F}^{-1}(2\sin(\alpha|f|^2))\mathcal{F}$$

Neglecting attenuation

b) Analytical reconstruction

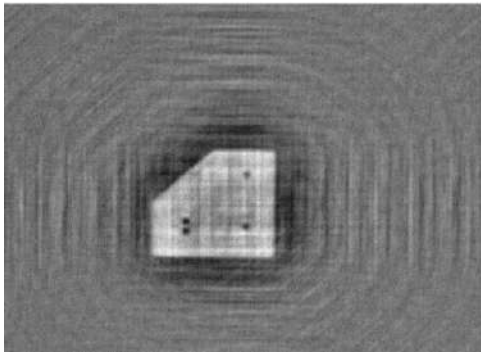

(c) ADMM reconstruction

- ADMM lagrangian.

$$\mathcal{L}(\phi, u, \alpha) = \frac{1}{2}\left|\left|H\phi - I\right|\right|_2^2 + \lambda\sum_i \left|\left|u_i\right|\right|_2 - \alpha^T(u - \nabla\phi) + \frac{\beta}{2}\left|\left|u - \nabla\phi\right|\right|_2^2$$

- ADMM iteratively minimizes L

  by solving smaller problems

Letter Vol. 42, No. 6 / March 15 2017 / Optics Letters

Optics Letters

Contrast-transfer-function phase retrieval based on compressed sensing

Pablo Villanueva-Perez,[1,4] Filippo Arcadu,[1,2,5] Peter Cloetens,[3] and Marco Stampanoni[1,2]

Sensitivity, resolution and photon flux

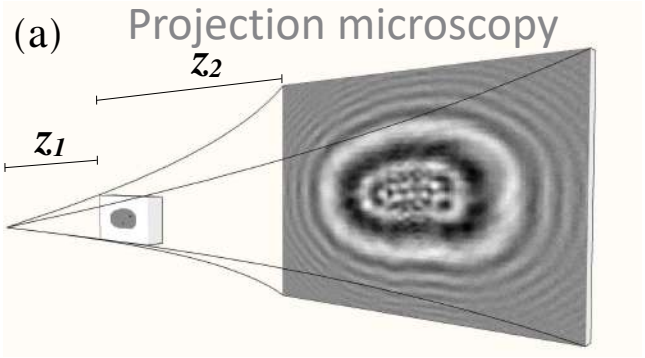

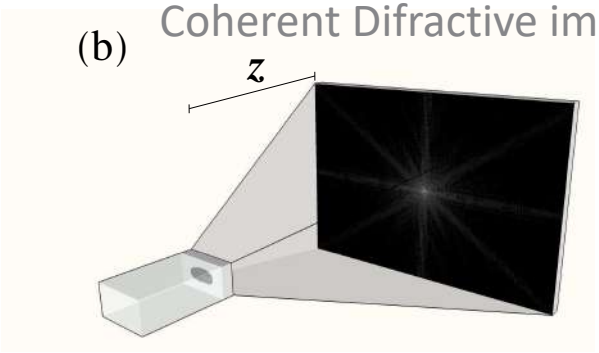

Total number of scattered photons

$$N_S = \Phi\sigma_S = \Phi \iint_{-\infty}^{+\infty} |1 - t(x,y)|^2 \mathrm{d}x\mathrm{d}y = \Phi\pi\sigma^2|\phi_{\max}|^2$$

Coherent flux

Total scattering cross section

Gaussian feature width

$$\mathrm{SNR}_{\mathrm{eff}}^{\mathrm{PM}} \equiv 2\sqrt{N_S\omega}|A| \simeq 2\sqrt{N_S}\frac{4}{\sqrt{\pi}}\beta\frac{2\sigma}{\mathrm{FOV}_{\mathrm{PM}}}$$

$$\mathrm{SNR}_{\mathrm{eff}}^{\mathrm{CDI}} \equiv \sqrt{N_S}\frac{2\sqrt{\pi}\sigma}{\mathrm{FOV}_{\mathrm{CDI}}}\frac{2\pi}{\pi q_{\max}^2}\int_0^{q_{\max}} e^{-\frac{\sigma^2 q^2}{2}} q\mathrm{d}q$$

$$\approx \sqrt{N_S}\frac{2\sigma}{\mathrm{FOV}_{\mathrm{CDI}}}\,.$$

Villanueva et al. Opt. Exp. 2016

Rajmund.Mokso@maxiv.lu.se

Sensitivity, resolution and photon flux

Resolution as a function of the maximum phase shift of the sample.

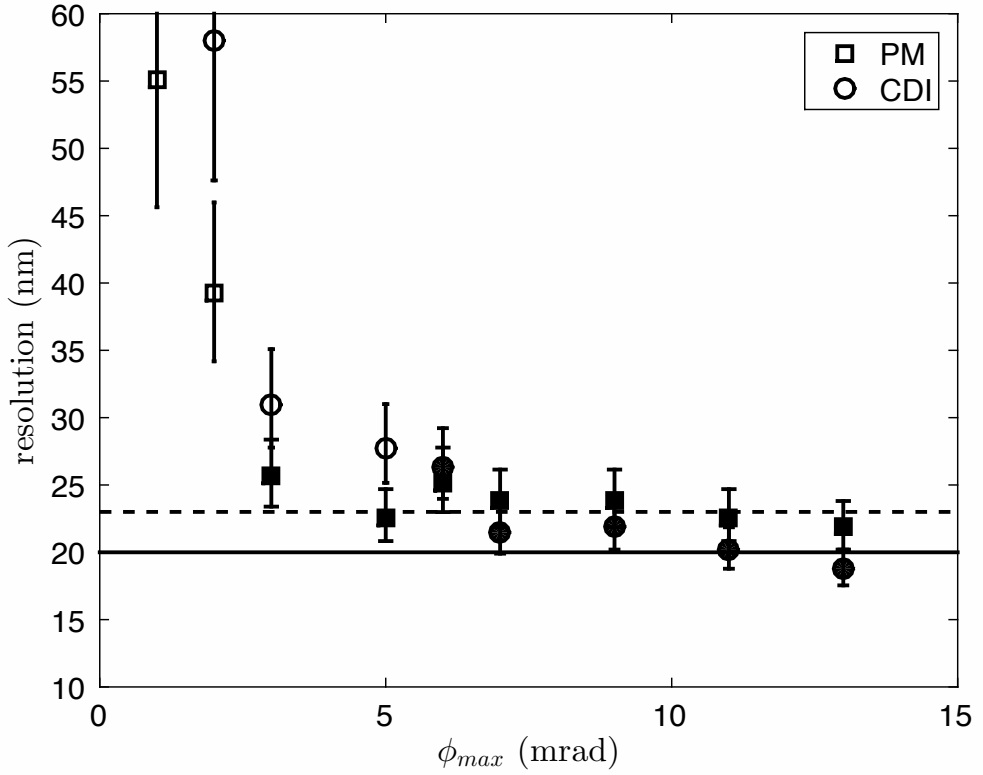

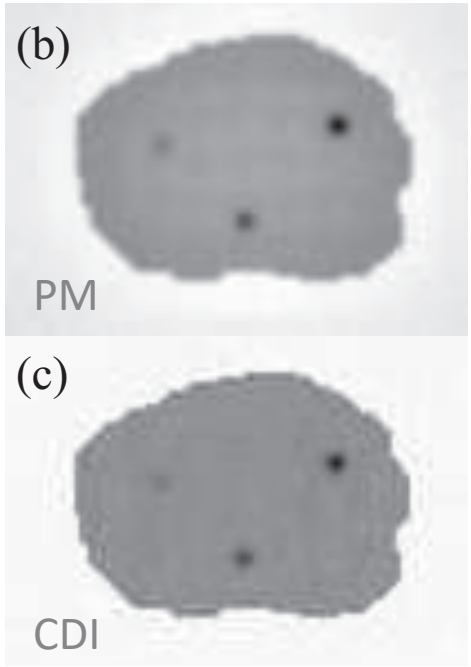

Villanueva et al. Opt. Exp. 2016

Rajmund.Mokso@maxiv.lu.se

Sensitivity, resolution and photon flux

The number of required photons is proportional to the desired spatial resolution.

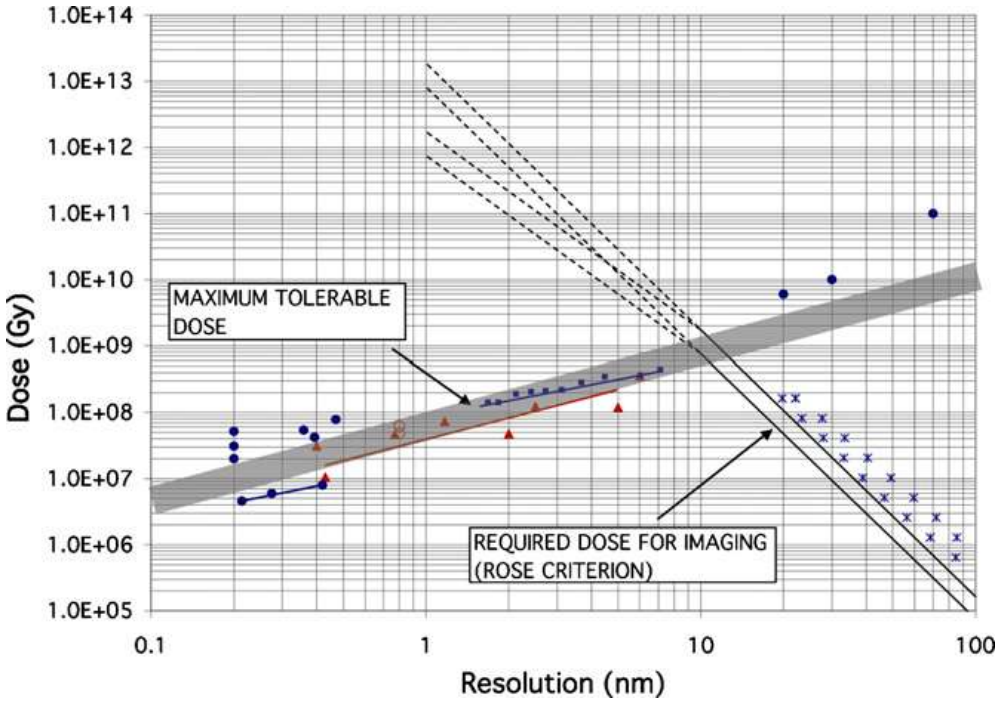

Howels et al., J. El.Spectr.2009

Required imaging fluence as a function of feature size (2σ)

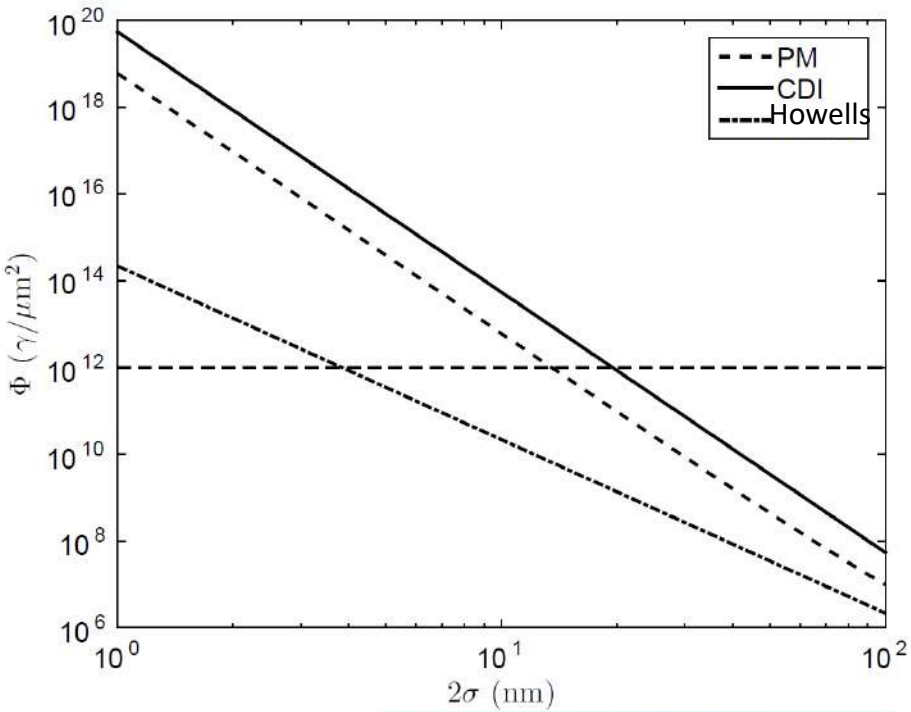

Villanueva et al. Opt. Exp. 2016

Total entrance dose

$$D[\mathrm{Gy}] = \phi \left(\frac{\mu}{\varrho}\right) \cdot h\nu \cdot t_{\mathrm{scan}}$$

$\phi \ldots$ flux [photons/s]

$h\nu \ldots$ energy per photon

$t_{\mathrm{scan}} \ldots$ total scan time

Rajmund.Mokso@maxiv.lu.se

Full-field imaging demo from MAX IV

See poster

NanoMAX experiment

Focus characterisation of the NanoMax Kirkpatrick-Baez mirror system

Markus Osterhoff[1], A.L. Robisch[1], S. Kalbfleisch[2], J. Soltau[1], M. Eckermann[1], D. Carbone[2], U. Johansson[2], T. Salditt[1]

[1] Institut für Röntgenphysik – Friedrich-Hund-Platz 1 – 37077 Göttingen, Germany
[2] MAX IV Laboratory – Lund University – Fotongatan 2 – 22484 Lund, Sweden

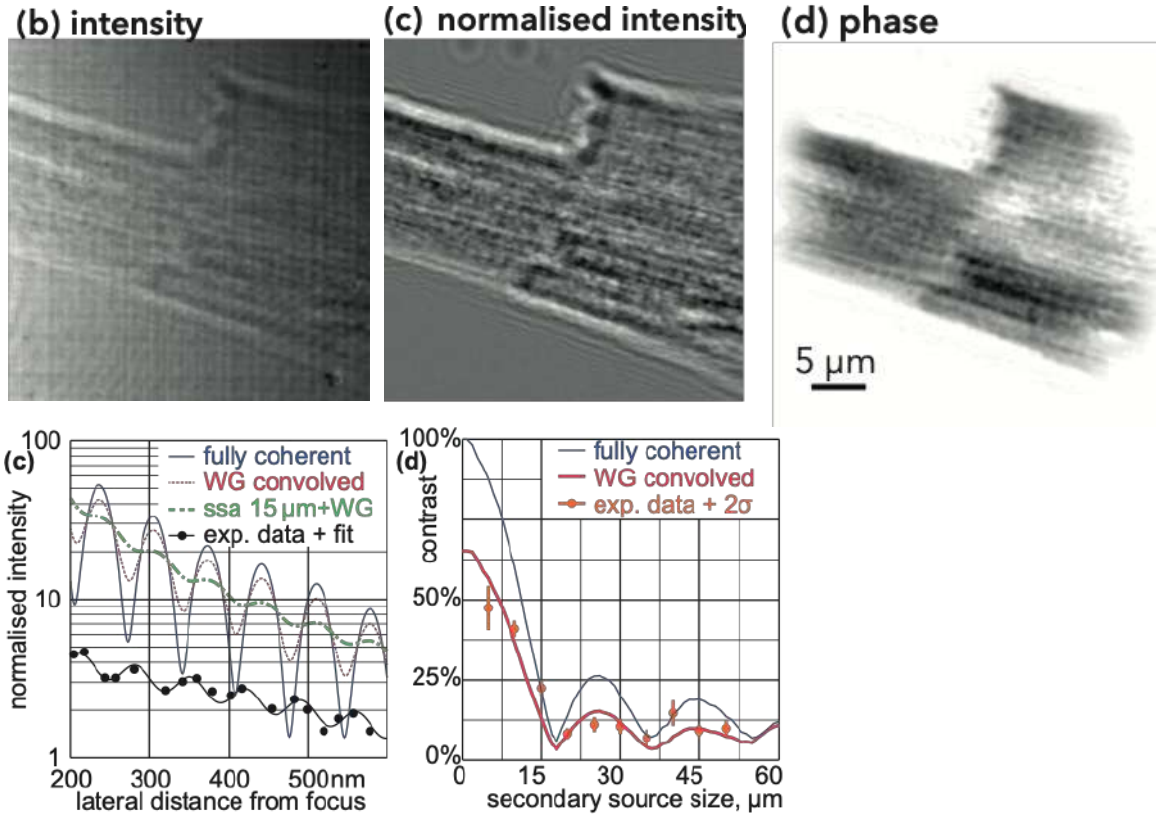

D.R. Luke: Relaxed averaged alternating reflections for diffraction imaging. Inverse Problems 21, 37 (2005)

(Fully) coherent beams

European XFEL

Highest coherence

Letter Vol. 6, No. 9 / September 2019 / Optica 1106

optica

Megahertz x-ray microscopy at x-ray free-electron laser and synchrotron sources

Patrik Vagovič,[1,2,3,*] Tokushi Sato,[1,2] Ladislav Mikeš,[2] Grant Mills,[2] Rita Graceffa,[2] Frans Mattsson,[4] Pablo Villanueva-Perez,[4,1] Alexey Ershov,[5] Tomáš Faragó,[5] Jozef Uličný,[6] Henry Kirkwood,[2] Romain Letrun,[2] Rajmund Mokso,[4] Marie-Christine Zdora,[7,8,9] Margie P. Olbinado,[10] Alexander Rack,[10] Tilo Baumbach,[5] Joachim Schulz,[2] Alke Meents,[1] Henry N. Chapman,[1] and Adrian P. Mancuso[2,11]

MHz radiography

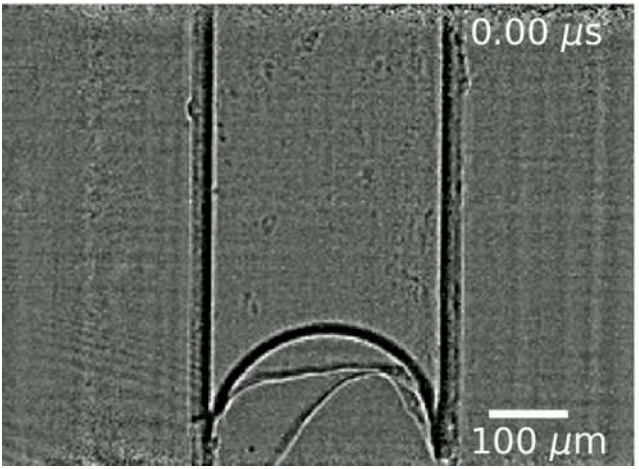

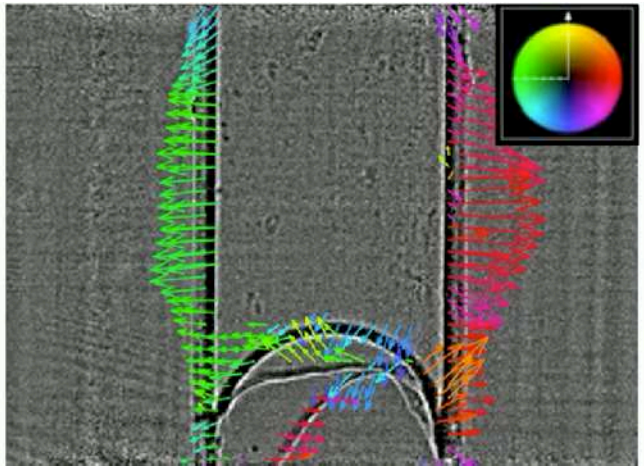

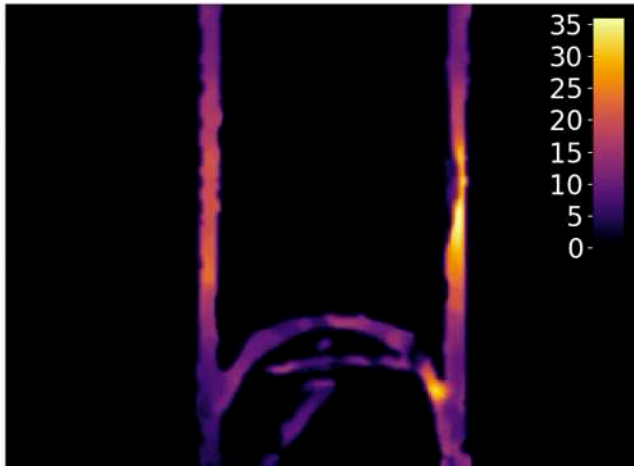

E = 9.3 keV,
the pulse train was filled with 128 x-ray pulses with a repetition rate of 1.128 MHz.
The effective pixel size of the imaging system was 3.2 µm

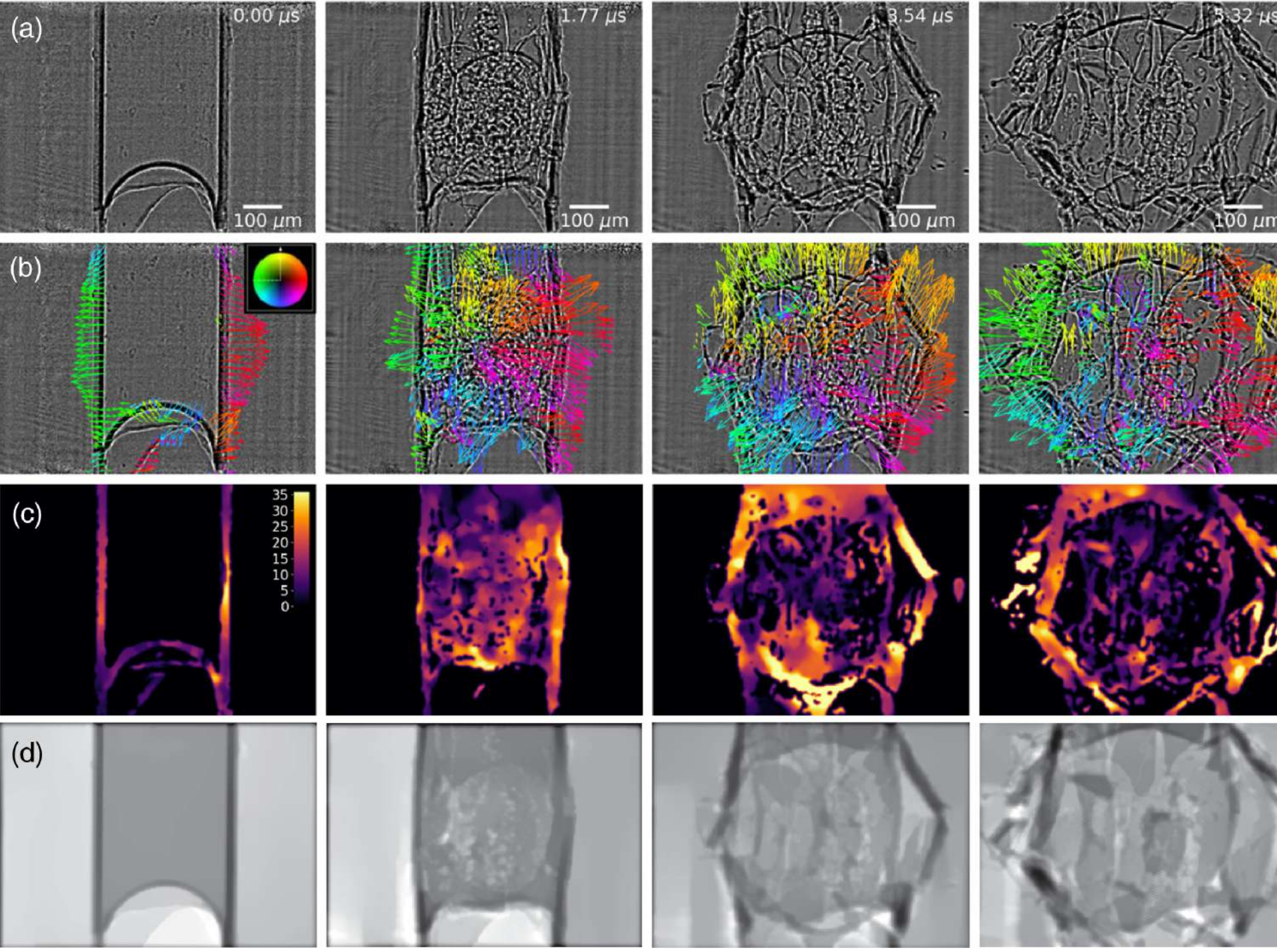
(a)
0.00 μs
100 μm
1.77 μs
100 μm
3.54 μs
100 μm
5.32 μs
100 μm
(b)
(c)
35
30
25
20
15
10
5
0
(d)

Challenges

Image reconstruction and analysis remains the bottleneck

Turning data into science

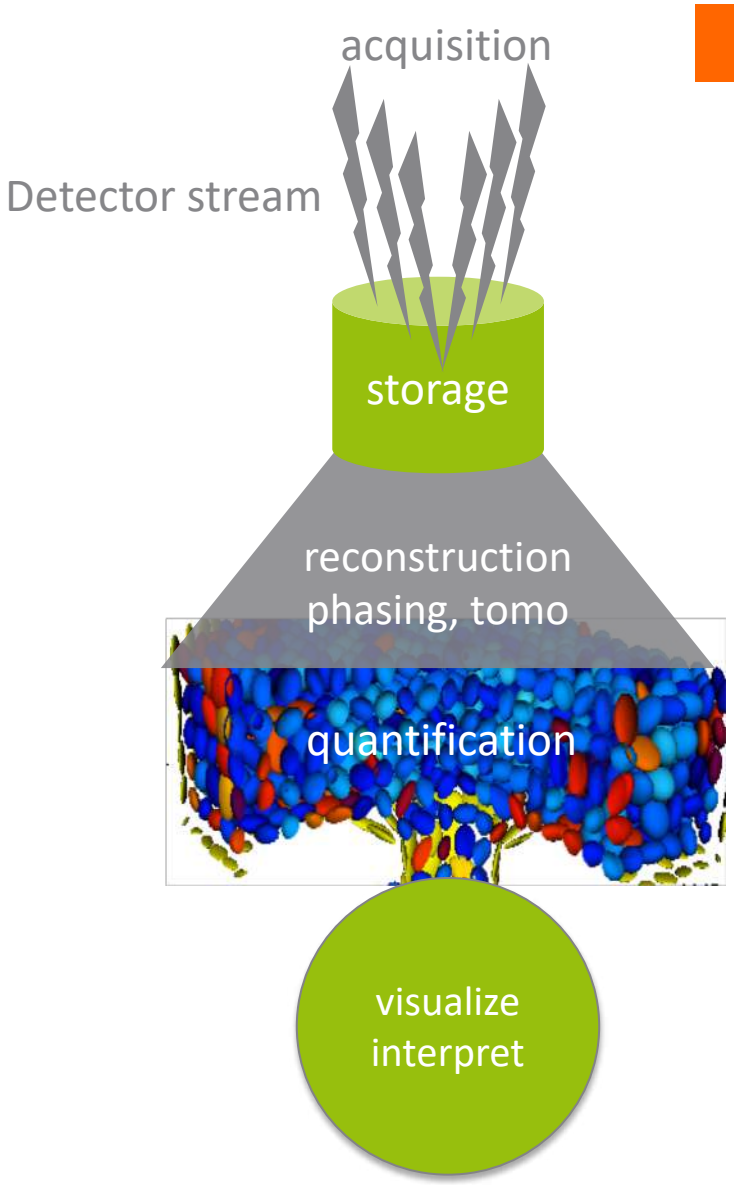

1TB / 2 min

300 GB

2 x 300 GB

1 GB

1 MB

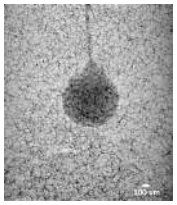

projections

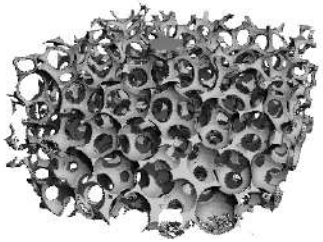

tomograms

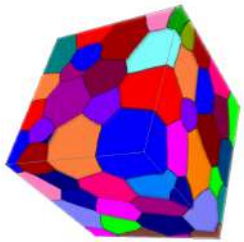

features

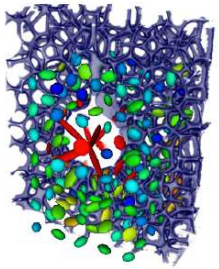

shapes

Rajmund.Mokso@maxiv.lu.se

MAXIV

Processing data streams for quality check and reduction

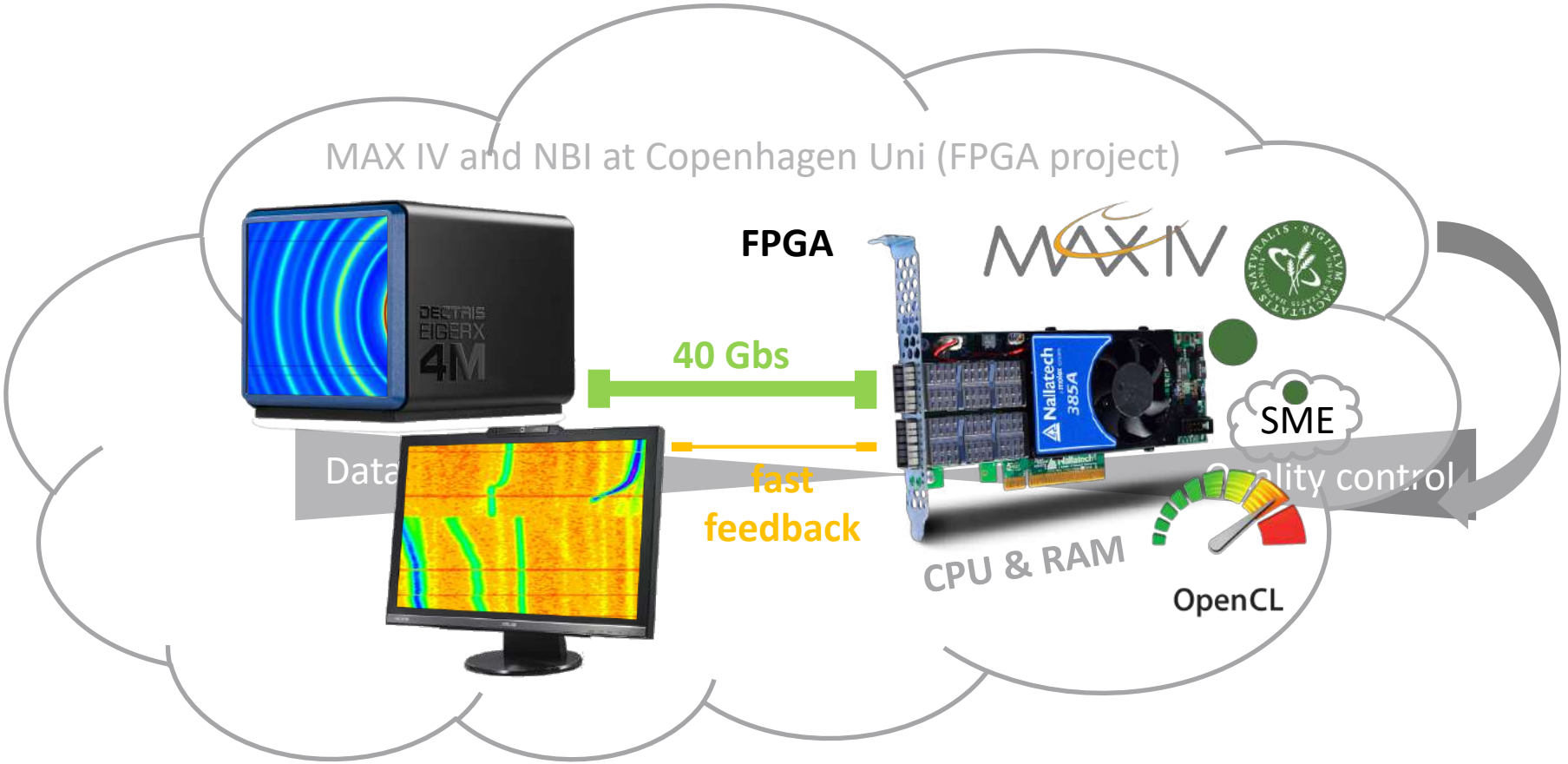

Data reduction in tomo: minimize number of scans saved per experiment.
E.g. foam dynamics studies contain lot of static scans. One could correlate consecutive 3D volumes and if they match one is deleted.

Dynamic tomographic reconstruction
Time domain decomposition

$$\mathcal{R}_\alpha f(s,z,\theta) = \iiint f(x,y,z,t)\delta(x\cos\theta + y\sin\theta - s)\delta(\theta - \alpha t)dx\,dy\,dt$$

Decomposition

$$f(x,y,z,t) \approx \sum_{j=0}^{M-1} f_j(x,y,z)\varphi_j(t),$$

where $\{f_j(x,y,z)\}_{j=0}^{M-1}$ are decomposition coefficients.

Example: Fourier basis $\varphi_j(t) = e^{2\pi i\, t\xi_j}$.

By using the linearity property of the projection operator:

$$\mathcal{R}_\alpha f(s,z,\theta) = \sum_{j=0}^{M-1} \mathcal{R} f_j(\theta,s,z)\varphi_j\left(\frac{\theta}{\alpha}\right)$$

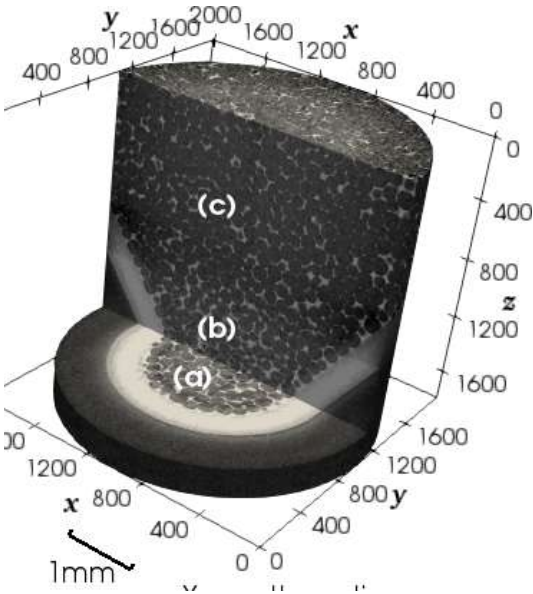

2016 x 2016 x 1800
130 rotations

$$\mathcal{R}_\alpha^* g(x,y,z,t) = \sum_{j=0}^{M-1} \varphi_j(t)\mathcal{R}^*\left(g\hat{\varphi}_j\right)(x,y,z),$$

where $\mathcal{R}, \mathcal{R}^*$ are standard projection and back-projection operators in the static case.

Dynamic tomography: ceramic particles

Tomography at 2BM, APS
2560 x 2560 x 700, 12 x 900 projections

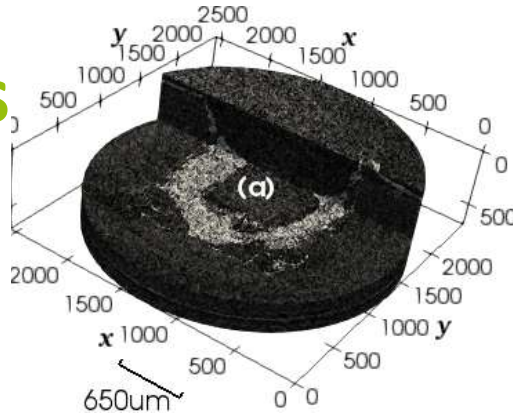

FBP reconstruction

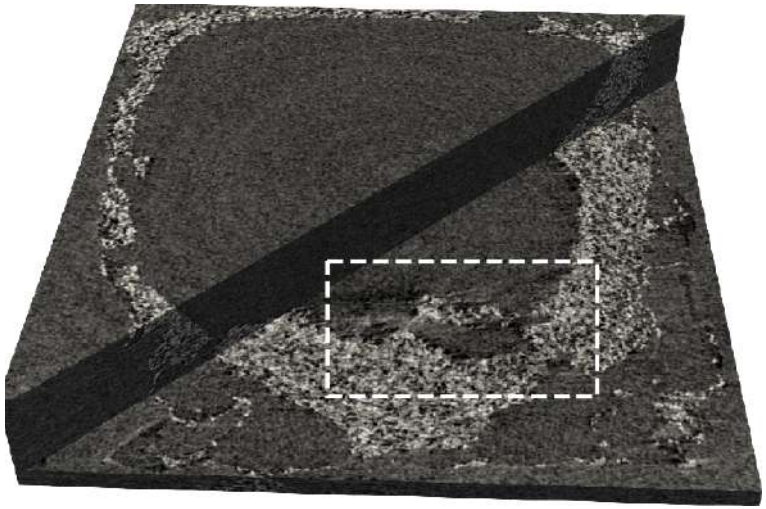

Iterative, basis size M=24

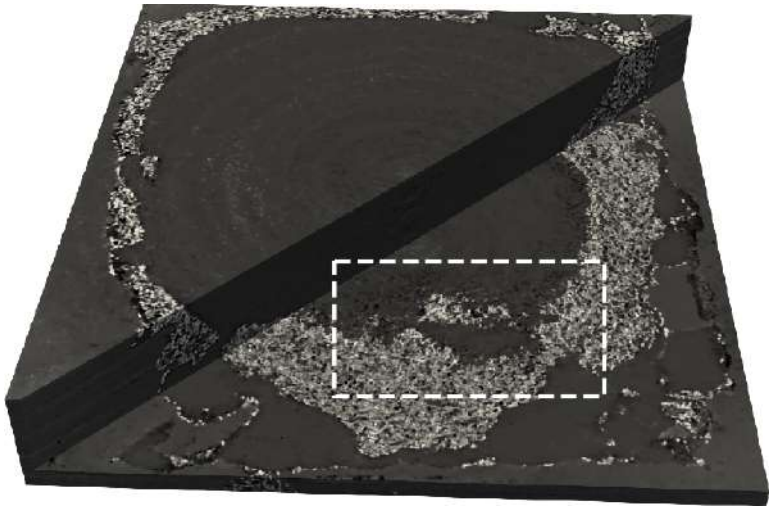

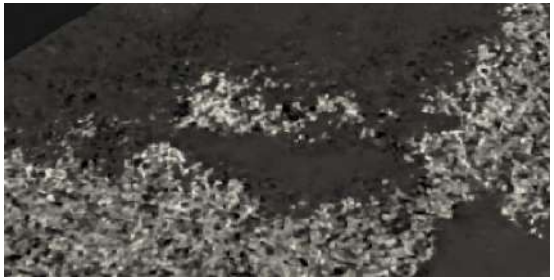

Rajmund.Mokso@maxiv.lu.se

… and here is how to use the new tool

Foam data https://tomobank.readthedocs.io

In this study, we investigate the rheology of liquid foams by fast synchrotron X-ray tomographic microscopy [B30]. Foams are complex cellular systems which require artifact free tomographic reconstruction for a reliable quantification of their time-dependent properties such as deformation fields of bubbles. In our example we acquire X-ray projections of the liquid foam flowing through a constriction and being rotated around the tomographic axis. The experiment was performed at the TOMCAT beamline of the Swiss Light Source using the fast acquisition setup [B28].

To load the data sets and perform reconstruction use the tomopy_rectv.py python script.

Reconstruction by Gridrec

```
python tomopy_rectv.py dk_MCFG_1_p_s1_.h5 --type subset --nsino 0.75 --binning 2 --frame 95
```

Reconstruction by the method with suppressing motion artifacts [Nikitin et. al, 2018] requires module *rectv* that can be installed from https://github.com/math-vrn/rectv_gpu. In this case, the algorithm run with option *-tv True*

```
python tomopy_rectv.py dk_MCFG_1_p_s1_.h5 --type subset --nsino 0.75 --binning 2 --tv True --frame
```

tomo_ID	00080
Image preview	
Downloads	tomo_00080
Instrument	SLS TOMCAT
Sample name	dk_MCFG_1_p_s1
Energy	16 keV
Sample-to-detector Distance	250 mm
Scan Range	180 degree

Rajmund.Mokso@maxiv.lu.se

MAXIV

Space for the missing tools

Complexity of the analysis

easy

middle

difficult

Off-line
- Interactive visualization and interactive scripting / annotation
- Feature quantification and visualization
- Vector field visualisation

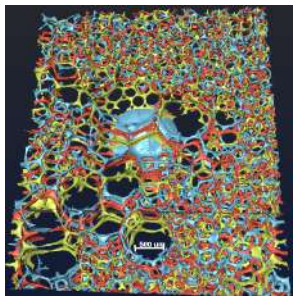

http://qim.compute.dtu.dk/

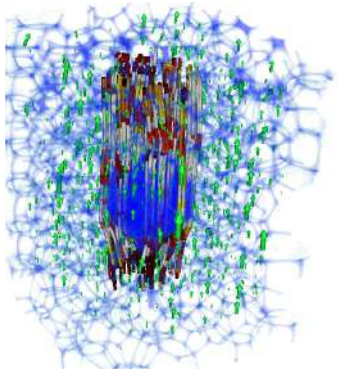

Streaming
- Detect changes in structure in real time (relate 2D to 3D)
- Interactive stream viewing (and decision taking)

seconds hours weeks

Time relative to experiment start

Rajmund.Mokso@maxiv.lu.se

Challenges

small field of view – large sample

High spatial resolution in large samples

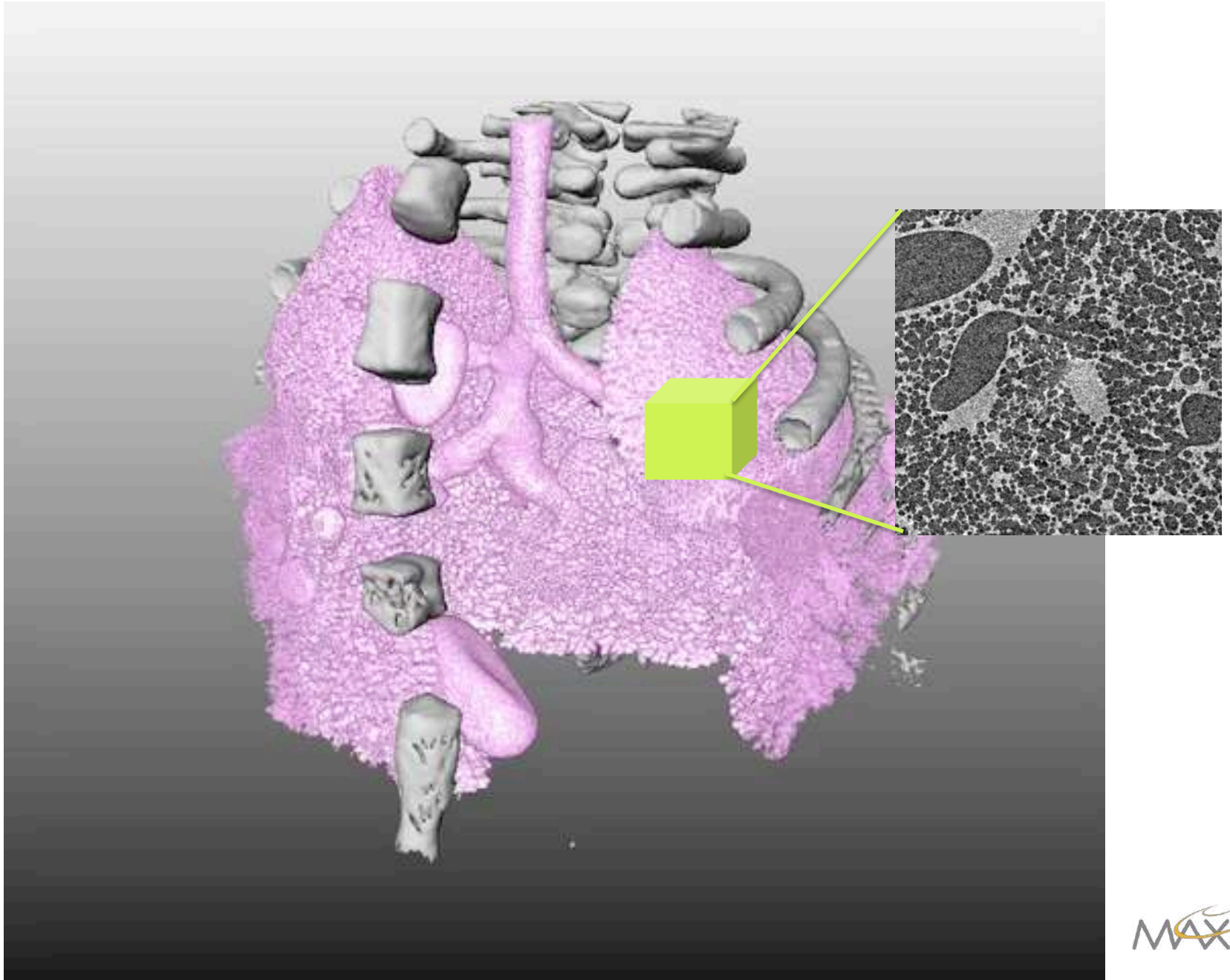

Local tomography: a multiresolution approach

Iterative reconstruction from combined high-low resolution sinogram pairs

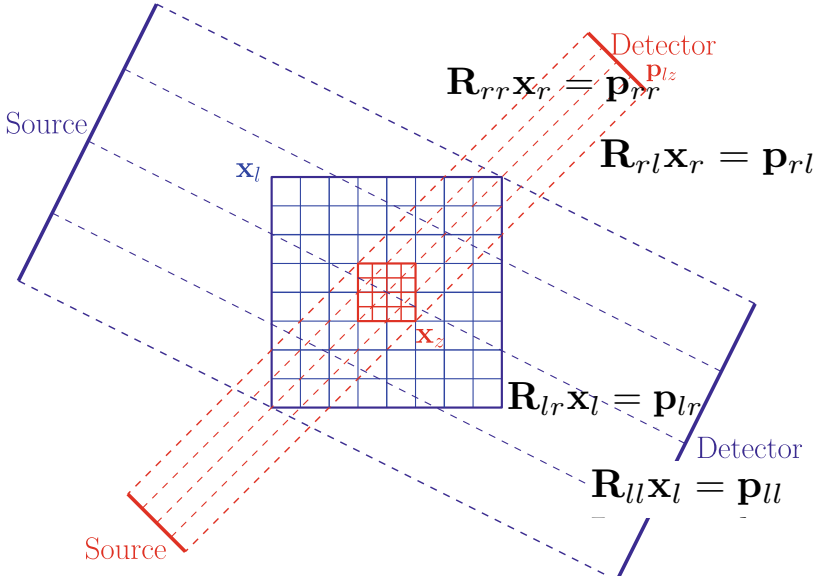

$$\mathbf{x}_r = \mathbf{y}_r + \mathbf{A}^T\mathbf{x}_l$$

Minimization of the energy function Which is convex => Adam gradient descent optimisation

Fidelity term in low. res.

Fidelity term in high. res.

$$\mathcal{E}(\mathbf{x}_l, \mathbf{y}_r) = \|\mathbf{R}_{ll}\mathbf{x}_l + \mathbf{R}_{rl}\mathbf{y}_r - \mathbf{p}_{ll}\|_2^2 + \|\mathbf{R}_{lr}\mathbf{x}_l + \mathbf{R}_{rr}\mathbf{y}_r - \mathbf{p}_{lr}\|_2^2 +$$

$$\gamma\|g(\mathbf{x}_l)\|_1 + \delta\|g(\mathbf{x}_r)\|_1 + \mu\|\mathbf{y}_r\|_1 + \nu\sum_{i=1}^{\omega_r^2}\sum_{j\in N_4(i)}|\mathbf{x}_r(i) - \mathbf{x}_r(j)|$$

positivity

Regularization of refinement image - noise

Smoothness regularization of 4-adjacent pixels of x_r

cost EUROPEAN COOPERATION IN SCIENCE & TECHNOLOGY

Varga & Mokso, Comp. Image Analysis, 2018

Rajmund.Mokso@maxiv.lu.se

MAXIV

Local tomography: a multiresolution approach

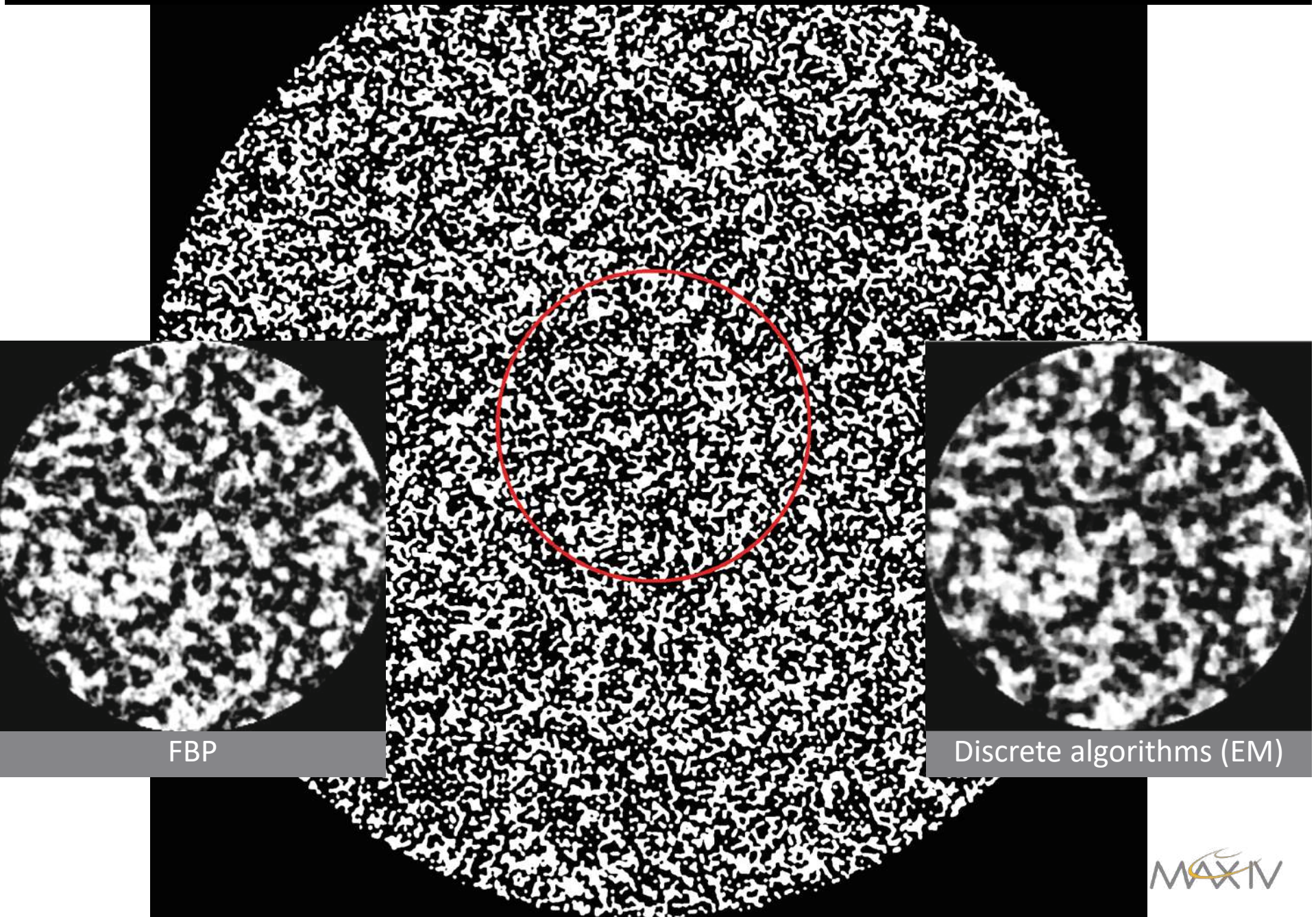


Perspectives
New science?

Fast tomographic microscopy: 3D

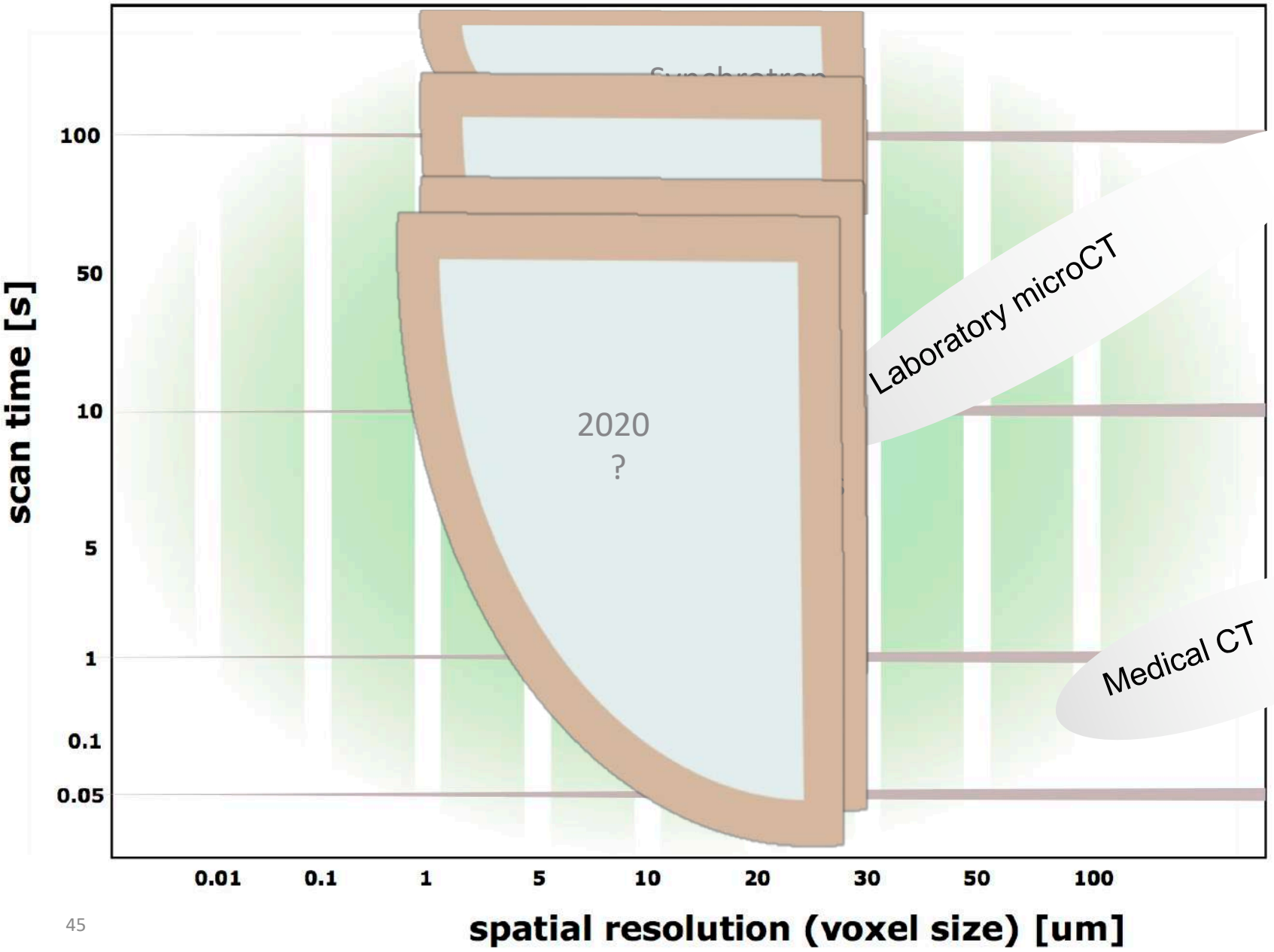

Real life system dynamics

nature COMMUNICATIONS

ARTICLE

https://doi.org/10.1038/s41467-019-11521-1 OPEN

Using X-ray tomoscopy to explore the dynamics of foaming metal

Francisco García-Moreno[1,2], Paul Hans Kamm[1,2], Tillmann Robert Neu[1,2], Felix Bülk[1,2], Rajmund Mokso[3], Christian Matthias Schlepütz[4], Marco Stampanoni[4,5] & John Banhart[1,2]

The rise of the Aluminum foam:
From nucleation to film rupture
Acquisition speed: 208 tomo / s
TOMCAT beamline, SLS

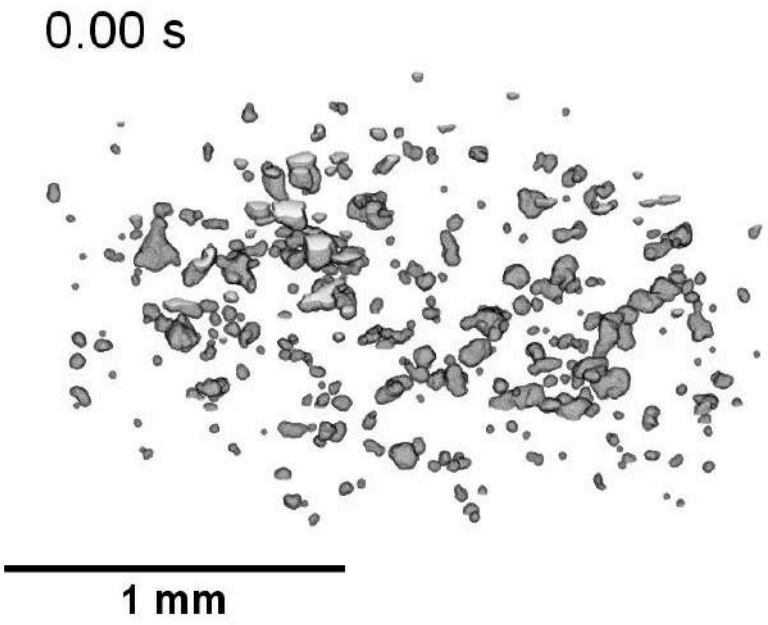

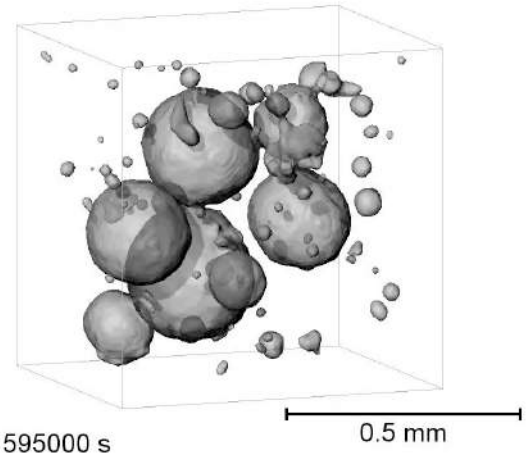

Exploiting new geometries: multiprojection

Realization of a 1:9 crystal splitter

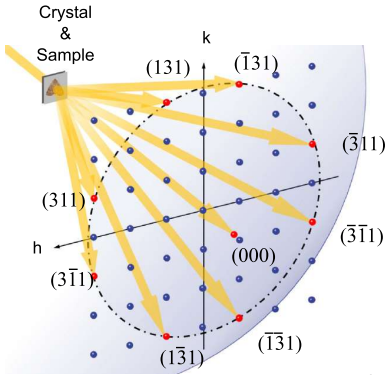

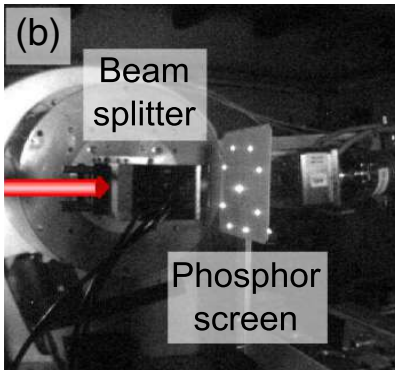

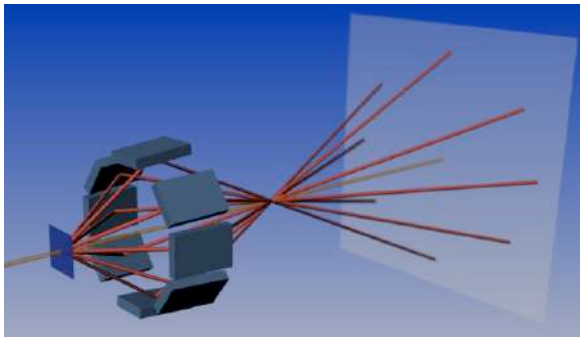

Far-field diffraction

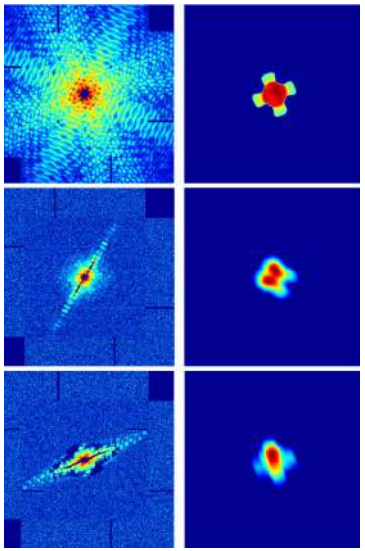

Near-field diffraction

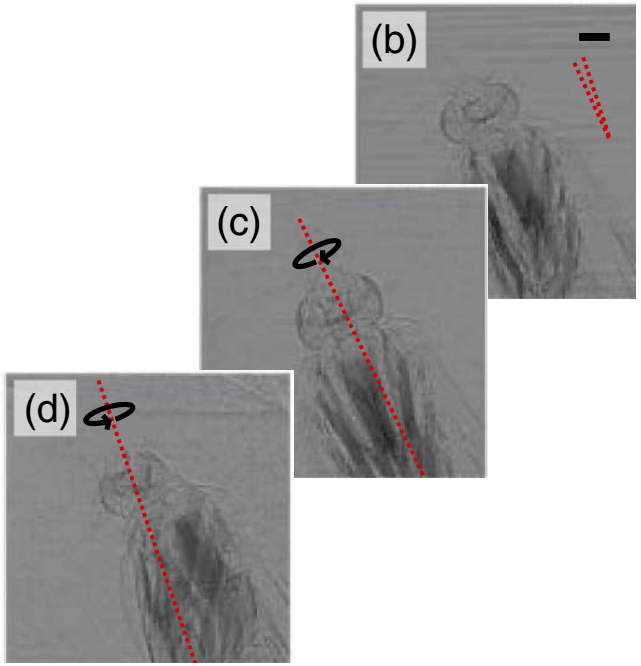

Joint project between Lund Uni, European XFEL, Berlin Uni.

Röntgen Ångström Cluster

optica

Hard x-ray multi-projection imaging for single-shot approaches

P. Villanueva-Perez,[1,2,*] B. Pedrini,[1] R. Mokso,[1,3] P. Vagovic,[2] V. A. Guzenko,[1] S. J. Leake,[4] P. R. Willmott,[1] P. Oberta,[5] C. David,[1] H. N. Chapman,[2,6,7] and M. Stampanoni[1,8]

MAX IV

Perspectives: shorter exposure times – less dose

Considerations for radiation dose optimization on the new sources:

- *Fringe visibility is proportional to the transversal coherence length at the sample position (= source size and distance). The contrast (CNR or SNR) comes through detecting the oscillation(s) of the Fresnel pattern.*
- *Phase retrieval algorithms perform better for samples with weak (no) attenuation => it makes sense to increase X-ray energy until the attenuation can be neglected (<5%)*
- *Looking into most efficient photon detection schemes on the optics / detector side (e.g. simultaneous 2 distance acquisition)*
- *Make use of modern tomographic reconstruction algorithms*

Deep sub-micron in vivo imaging of photoreceptor movement in drosophila
100 fps @ ID16B

Mikko Juusola
University of Scheffield

Evidence for high resolution stereovision in compound eyes

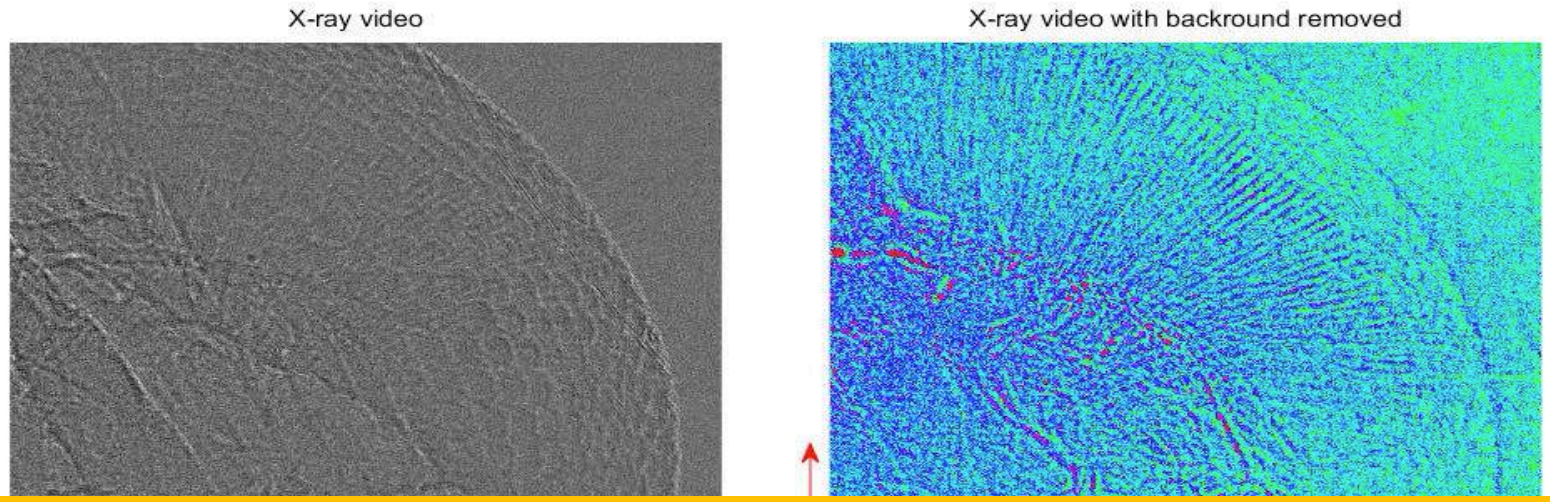

For reliable scientific interpretation In vivo measurement must be complemented by nanotomography with highest possible accuracy (cryo-nanotomo)

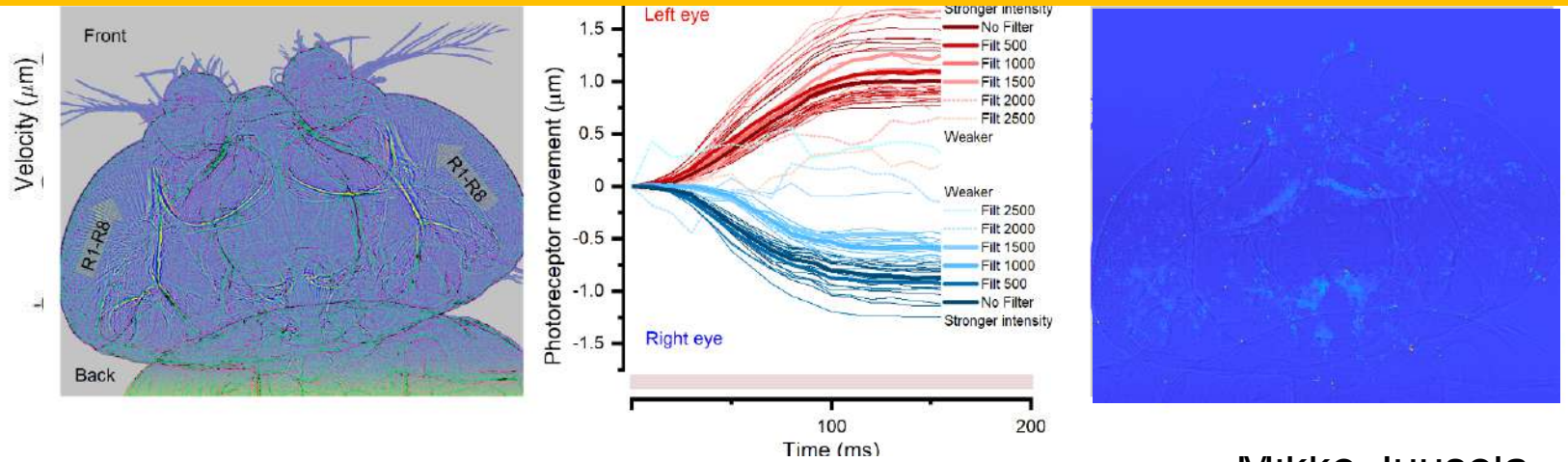

Mikko Juusola
University of Scheffield

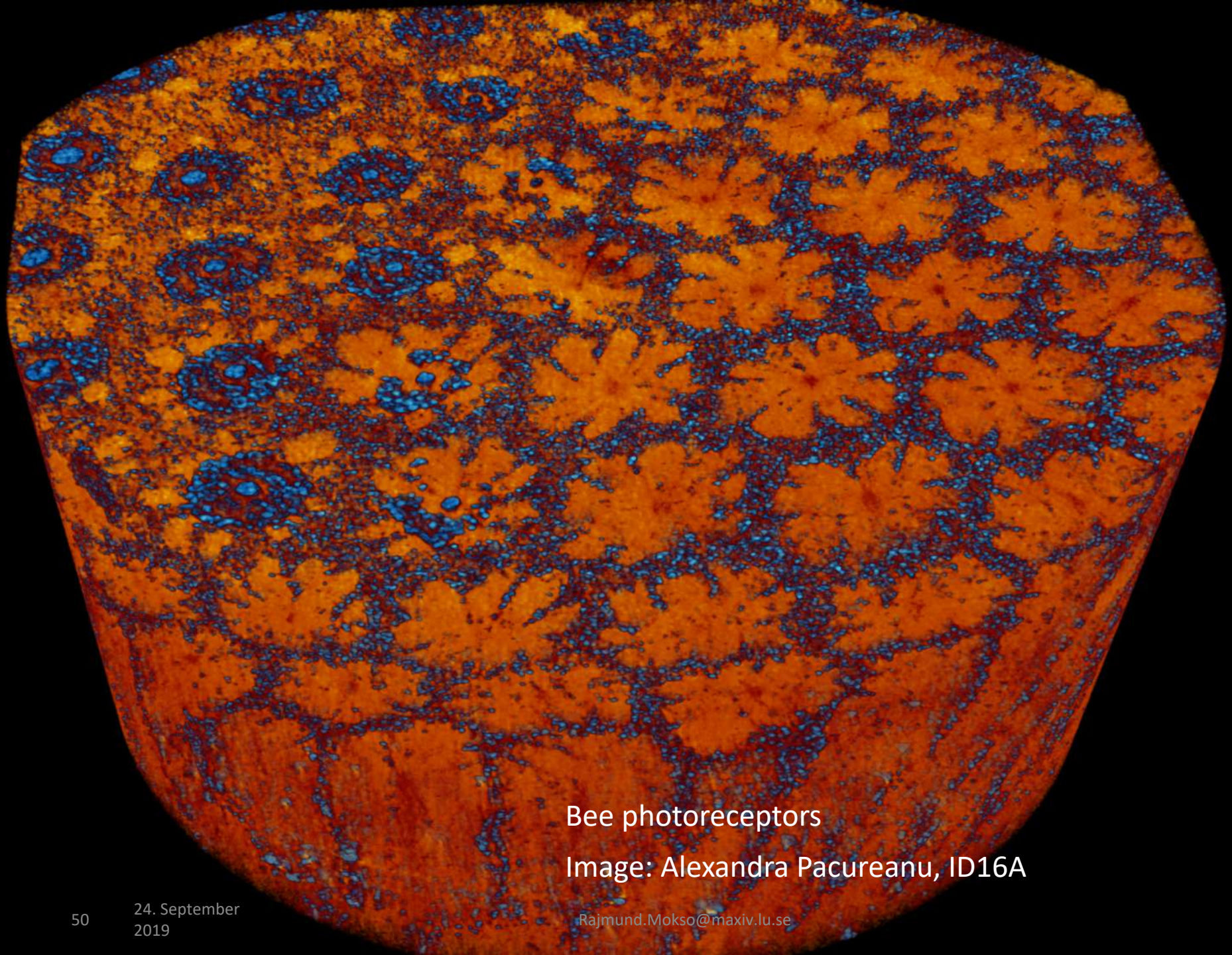

Bee photoreceptors

Image: Alexandra Pacureanu, ID16A

Rajmund.Mokso@maxiv.lu.se

Perspectives: new science?

3D histology (in vivo)

- Image 3D living tissue at the cellular level in 3D

Nanoscale characterization of materials with realistic dimensions

- Pores, defects

Exploiting new phasing methods: convolutional neural networks

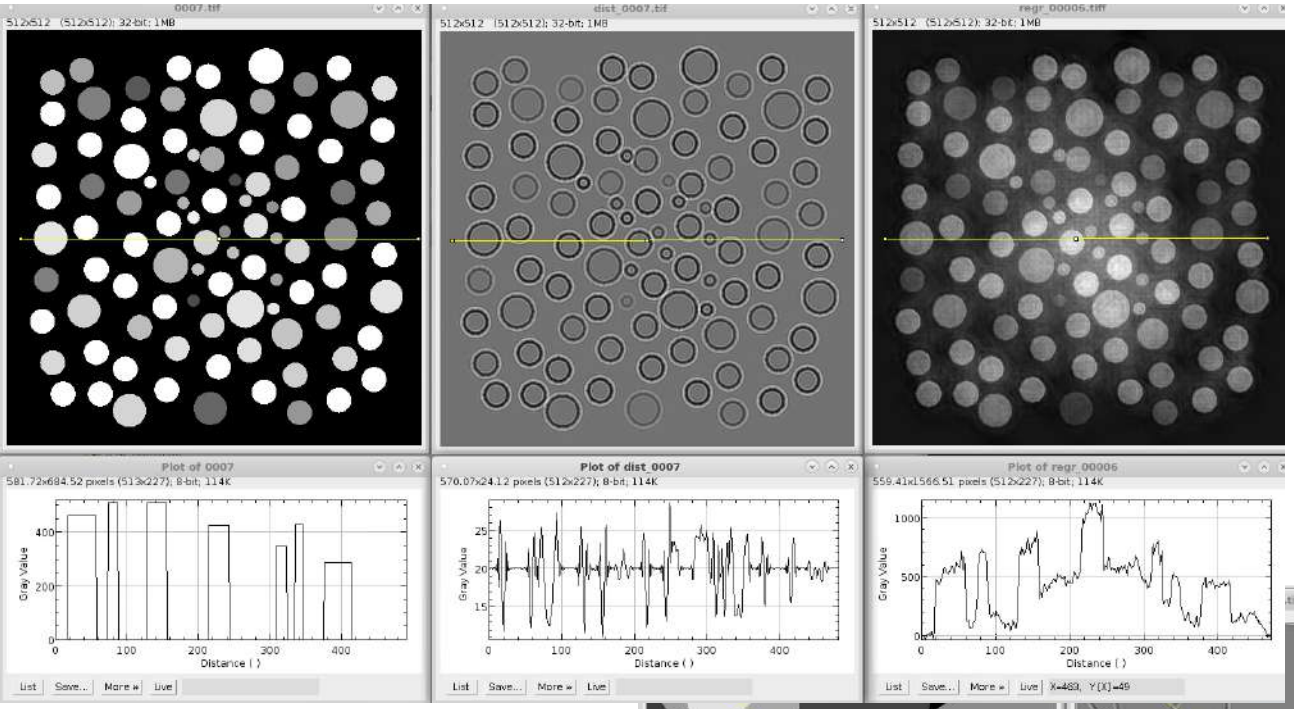

D. Figueras, summer project @ MAX IV

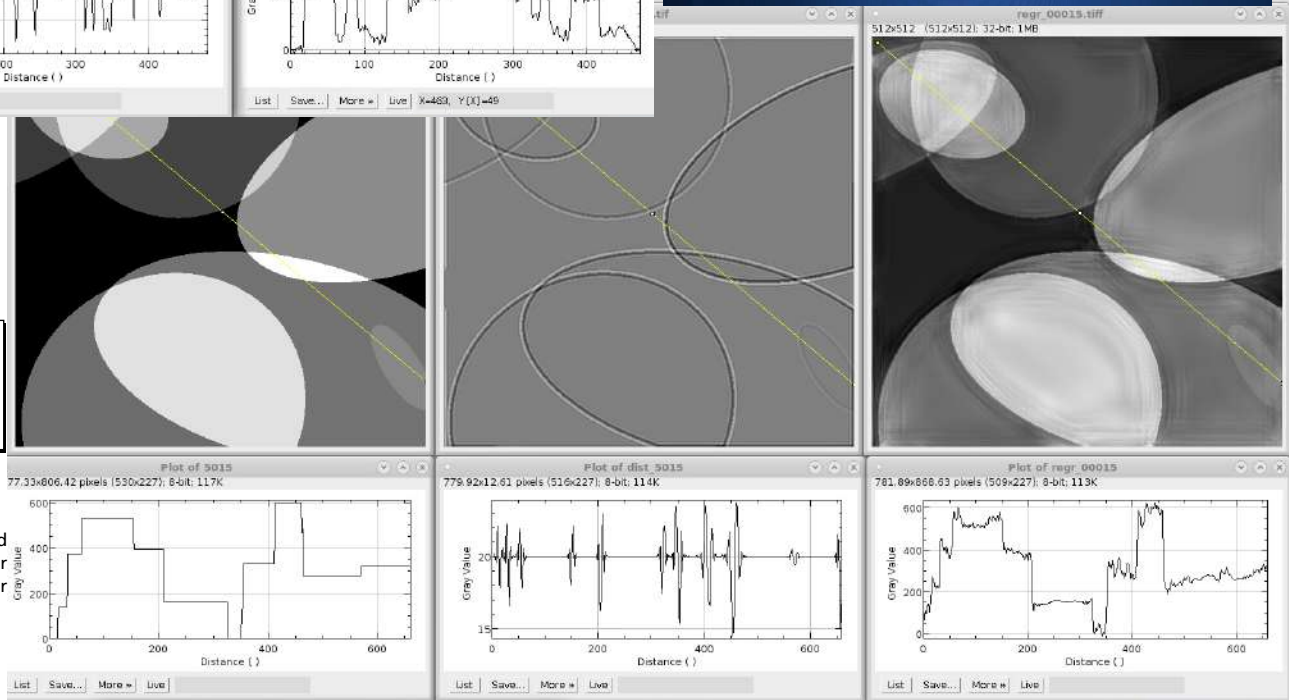

D. Pelt & J. Sethian, Mixed-scale dense CNN for image analysis, PNAS 115, 2018

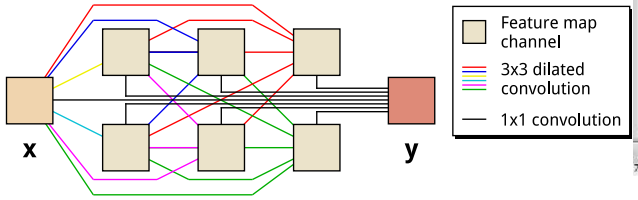

Fig. 3. Schematic representation of an MS-D network with $w = 2$ and $d = 3$. Colored lines represent 3×3 dilated convolutions, with each color representing a different dilation. Note that all feature maps are used for

Phase retrieval: Bayesian approach

Projection microscopy, ID16

Probability density functions are assigned to this quantities: $p(\mathbf{x})$ as the prior distribution, $p(\mathbf{y}|\mathbf{x})$ as the likelihood and $p(\mathbf{x}|\mathbf{y})$ as the the posterior distribution. Applying the Bayes rule for probabilities [24], the posterior distribution is found to be proportional to the multiple of the previous two:

$$p(\mathbf{x}|\mathbf{y}) = \frac{p(\mathbf{y}|\mathbf{x})\ p(\mathbf{x})}{p(\mathbf{y})} \propto p(\mathbf{y}|\mathbf{x})\ p(\mathbf{x}), \tag{30}$$

where the denominator $p(\mathbf{y}) = \int p(\mathbf{y}|\mathbf{x})\, p(\mathbf{x})\, \mathrm{d}x$ is a normalizing constant called evidence, that will be ignored in the following formalism.

Let's consider a white noise distribution for $\boldsymbol{\epsilon}$, $p(\boldsymbol{\epsilon}) = \mathcal{N}(\boldsymbol{\epsilon}|0, v_\epsilon \mathbf{I})$, i.e. a Gaussian distribution with zero mean and where v_ϵ denotes the variance of the noise. In turn the likelihood follows a Gaussian distribution of mean equal to the model simulation $\mathbf{Hx}$ and variance equal to that of the noise:

$$p(\mathbf{y}|\mathbf{x}) = \mathcal{N}(\mathbf{y}|\mathbf{Hx}, v_\epsilon \mathbf{I}) \propto v_\epsilon^{-\frac{M}{2}} \exp\{-\frac{1}{2v_\epsilon}\|\mathbf{y} - \mathbf{Hx}\|^2\}. \tag{31}$$

In the case of *maximum a posteriori* (MAP) estimation of the posterior distribution $p(\mathbf{x}, \boldsymbol{\theta}|\mathbf{y})$ the Bayesian approach [25] is able to infer on both the unknown quantity $\mathbf{x}$ and the hyper-parameters of the model, $\boldsymbol{\theta}$:

$$\begin{aligned} \hat{\mathbf{x}} &= \arg\max_{\mathbf{x}} p(\mathbf{x}, \boldsymbol{\theta}|\mathbf{y}) = \arg\min_{\mathbf{x}} J(\mathbf{x}), \quad \text{where } J(\mathbf{x}) = -\ln p(\mathbf{x}, \boldsymbol{\theta}|\mathbf{y}), \\ \hat{\boldsymbol{\theta}} &= \arg\max_{\boldsymbol{\theta}} p(\mathbf{x}, \boldsymbol{\theta}|\mathbf{y}) = \arg\min_{\boldsymbol{\theta}} J(\mathbf{x}) \end{aligned} \tag{34}$$

Summary

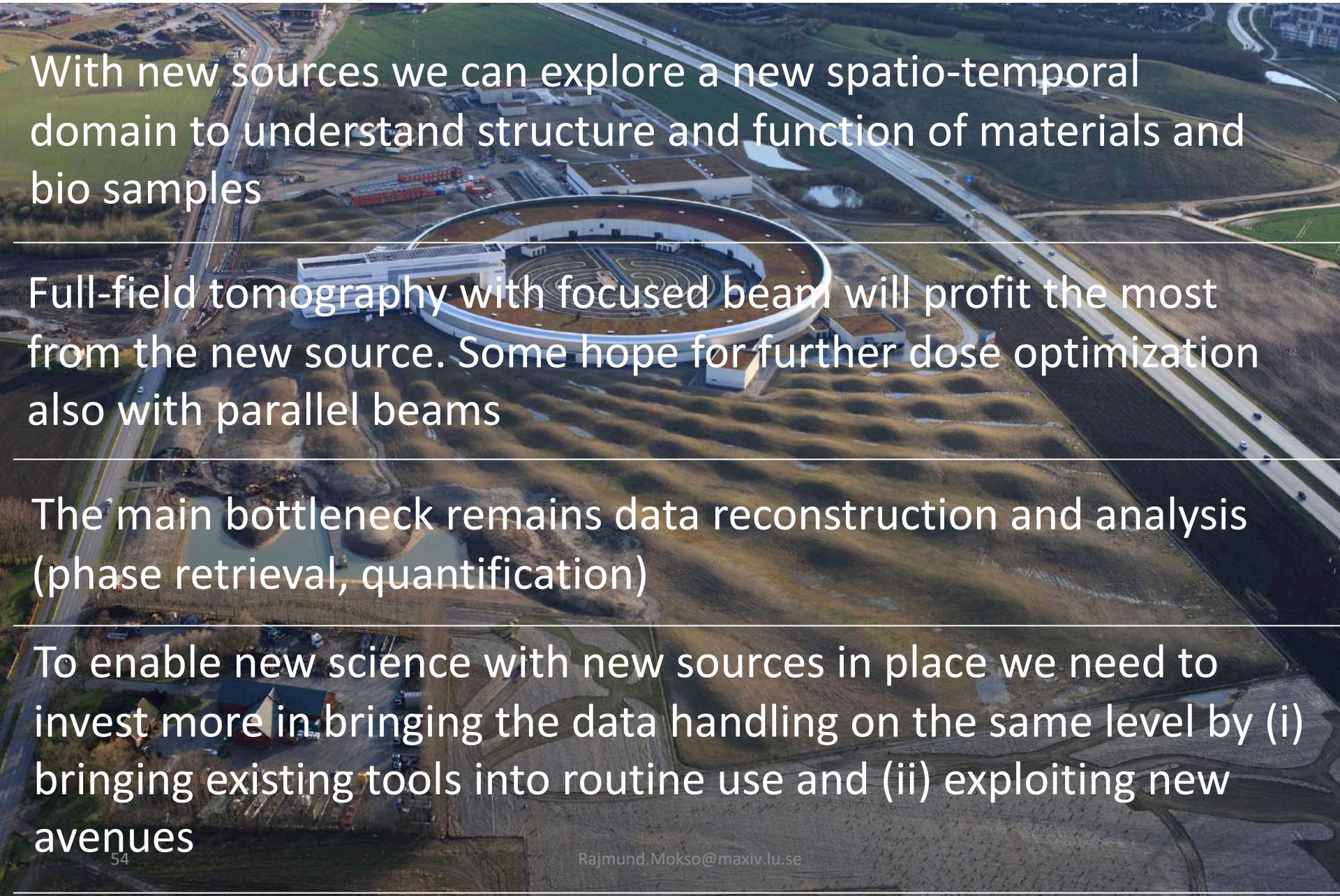

With new sources we can explore a new spatio-temporal domain to understand structure and function of materials and bio samples

Full-field tomography with focused beam will profit the most from the new source. Some hope for further dose optimization also with parallel beams

The main bottleneck remains data reconstruction and analysis (phase retrieval, quantification)

To enable new science with new sources in place we need to invest more in bringing the data handling on the same level by (i) bringing existing tools into routine use and (ii) exploiting new avenues

Rajmund.Mokso@maxiv.lu.se


Thank you!